Chapter 1
The Radiation Damage Event

The radiation damage event is defined as the transfer of energy from an incident projectile to the solid and the resulting distribution of target atoms after completion of the event. The radiation damage event is actually composed of several distinct processes. These processes and their order of occurrence are as follows:

1. The interaction of an energetic incident particle with a lattice atom.
2. The transfer of kinetic energy to the lattice atom giving birth to a primary knock-on atom (PKA).
3. The displacement of the atom from its lattice site.
4. The passage of the displaced atom through the lattice and the accompanying creation of additional knock-on atoms.
5. The production of a displacement cascade (collection of point defects created by the PKA).
6. The termination of the PKA as an interstitial.

The radiation damage event is concluded when the PKA comes to rest in the lattice as an interstitial. The result of a radiation damage event is the creation of a collection of point defects (vacancies and interstitials) and clusters of these defects in the crystal lattice. It is worth noting that this entire chain of events consumes only about 10^{-11} s (see Table 1.1). Subsequent events involving the migration of the point defects and defect clusters and additional clustering or dissolution of the clusters are classified as *radiation damage effects*.

What we first need to know in order to understand and quantify radiation damage is how to describe the interaction between a particle and a solid that produces displacements, and later on how to quantify this process. The most simple model is one that approximates the event as colliding hard spheres with displacement occurring when the transferred energy is high enough to knock the struck atom off its lattice site. In addition to energy transfer by hard sphere collisions, the moving atom loses energy by interactions with electrons, the Coulomb field of nearby atoms, the periodicity of the crystalline lattice, etc. The problem is reduced to the following. If we can describe the energy-dependent flux of the incident particle and the energy transfer cross sections (probabilities) for collisions between atoms, then we can quantify the PKA production in a differential energy range and utilize this to determine the number of displaced atoms.

G.S. Was, *Fundamentals of Radiation Materials Science*,
DOI 10.1007/978-1-4939-3438-6_1

Table 1.1 Approximate timescale for the production of defects in irradiated metals (from [1])

Time (s)	Event	Result
10^{-18}	Energy transfer from the incident particle	Creation of a primary knock-on atom (PKA)
10^{-13}	Displacement of lattice atoms by the PKA	Displacement cascade
10^{-11}	Energy dissipation, spontaneous recombination, and clustering	Stable Frenkel pairs (single interstitial atoms (SIA) and vacancies) and defect clusters
$>10^{-8}$	Defect reactions by thermal migration	SIA and vacancy recombination, clustering, trapping, defect emission

In this chapter, we will concentrate on quantifying the energy transferred between interacting bodies as well as describing the energy transfer cross section. We will begin with neutron–nucleus reactions since the neutrality of the neutron makes the interaction particularly straightforward. Following creation of the PKA, subsequent interactions occur between atoms, and the positive charge of the nucleus and the negative charge of the electron cloud become important in understanding how atoms interact. In fact, atom–atom interaction is the low-energy limit of ion–atom interactions that occur in reactor cores and via ion irradiation using accelerators over a wide energy range and can lead to the last type of interaction: ionization collisions.

1.1 Neutron–Nucleus Interactions

1.1.1 Elastic Scattering

By virtue of their electrical neutrality, elastic collisions between neutrons and nuclei can be represented as colliding hard spheres. When neutrons pass through a solid, there is a finite probability that they will collide with a lattice atom, imparting a recoil energy to the struck atom. This probability is defined by the double differential scattering cross section (in energy and angle), σ_s (E_i, E_f, Ω), where E_i and E_f are the incident and final energies and Ω is the solid angle into which the neutron is scattered. We are often only interested in the scattering probability as a function of E_i and the scattering angle. The single differential scattering cross section is as follows:

$$\sigma_s(E_i, \Omega) = \int \sigma_s(E_i, E_f, \Omega) \mathrm{d}E_f. \tag{1.1}$$

The total scattering probability for neutrons of energy E_i is as follows:

$$\sigma_s(E_i) = \int \sigma_s(E_i, \Omega) \mathrm{d}\Omega. \tag{1.2}$$

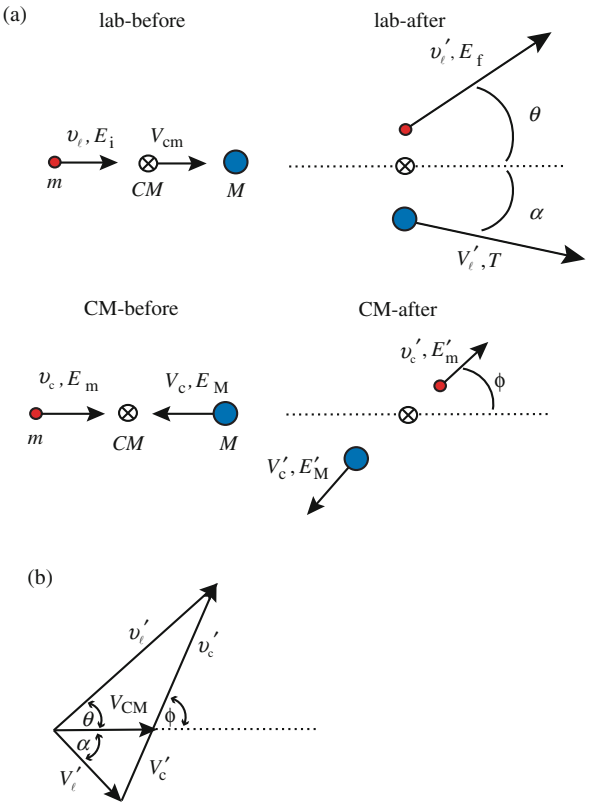

Fig. 1.1 Vector velocities (**a**) in the laboratory and center-of-mass (CM) systems and (**b**) composite diagram relating velocities in the two systems

In the study of irradiation effects, we are interested in the behavior of the struck atom. So we are seeking σ_s (E_i, T); the energy transfer cross section, or the probability that a neutron of energy E_i elastically scattering against an atom of mass M, will impart a recoil energy T to the struck atom. But first it is necessary to find T in terms of the neutron energy and the scattering angle. To do this, let us consider the dynamics of binary elastic collisions in the center-of-mass and laboratory frames.

Figure 1.1(a) shows the trajectories of a neutron and the target nucleus before and after scattering, as seen from both the laboratory reference system and the center-of-mass system. The easiest way to obtain a relationship between the incident neutron energy, scattering angle, and transferred energy is to analyze the dynamics of the collision in the center-of-mass (CM) system. When the collision is viewed in the center-of-mass system, the recoiling particles appear to move away from each other in opposite directions. Momentum conservation along the axes of approach and departure yields the following:

$$\begin{aligned} \upsilon_c m - V_c M &= 0 \\ \upsilon'_c m - V'_c M &= 0, \end{aligned} \tag{1.3}$$

and conservation of kinetic energy requires that:

$$\frac{1}{2}mv_c^2 + \frac{1}{2}MV_c^2 = \frac{1}{2}mv_c'^2 + \frac{1}{2}MV_c'^2. \tag{1.4}$$

Using Eq. (1.3) to eliminate v_c and v_c', we get:

$$\left[\frac{1}{2}m\left(\frac{M}{m}\right)^2 + \frac{1}{2}M\right]V_c^2 = \left[\frac{1}{2}m\left(\frac{M}{m}\right)^2 + \frac{1}{2}M\right]V_c'^2. \tag{1.5}$$

Therefore,

$$\begin{aligned} V_c &= V_c', \text{ and hence,} \\ v_c &= v_c'. \end{aligned} \tag{1.6}$$

Since the target nucleus is at rest in the laboratory system and moving to the left with speed V_c in the CM system, the CM system itself must be moving to the right relative to the laboratory system with the same speed, V_c. Thus, if we use V_{CM} to denote the speed of the CM system relative to the laboratory system, the magnitudes of V_{CM} and V_c are the same (but opposite in direction). This can be restated as follows:

$$v_c = v_\ell - V_{CM} = v_\ell - V_c, \tag{1.7}$$

and using Eq. (1.3), we find that:

$$V_{CM} = \left(\frac{m}{M+m}\right)v_\ell. \tag{1.8}$$

Recall that we want to relate T, the energy transferred to the struck atom, to ϕ, the scattering angle in the CM system. Using vector addition, we can relate the recoil target nucleus velocity in the laboratory system, V_ℓ', to ϕ as shown in Fig. 1.1(b), which is a composite of the interaction in the laboratory and CM systems as shown in Fig. 1.1(a). Using the law of cosines:

$$V_\ell'^2 = V_{CM}^2 + V_c'^2 - 2V_{CM}V_c'\cos\phi, \tag{1.9}$$

and rewriting the velocities in Eq. (1.9) in terms of energy gives:

$$V_\ell'^2 = \frac{2T}{M}, \quad V_{CM}^2 = \frac{2E_i}{m}\left(\frac{m}{m+M}\right)^2, \quad \text{and} \quad V_c'^2 = \frac{2m}{M^2}E_m',$$

and substituting these expressions into Eq. (1.9) gives:

$$T = \frac{mM}{(m+M)^2} E_\mathrm{i} + \frac{m}{M} E'_\mathrm{m} - 2\left(\frac{m}{m+M}\right)(E_\mathrm{i} E'_\mathrm{m})^{1/2} \cos\phi, \tag{1.10a}$$

or

$$T = \eta_1 \eta_2 E_\mathrm{i} + \frac{\eta_1}{\eta_2} E'_\mathrm{m} - 2\eta_1 (E_\mathrm{i} E'_\mathrm{m})^{1/2} \cos\phi, \tag{1.10b}$$

where $\eta_1 = m/(m + M)$ and $\eta_2 = M/(m + M)$.

Since we want to find the energy transferred, T, as a function of initial energy and scattering angle only, we use the relationship between E_i and E'_m to eliminate E'_m. From Eqs. (1.7) and (1.8), we know that:

$$\upsilon'_\mathrm{c} = \upsilon_\ell - \left(\frac{m}{m+M}\right)\upsilon_\ell = \upsilon_\ell \left(\frac{M}{m+M}\right). \tag{1.11}$$

Writing Eq. (1.11) in terms of energy gives:

$$E'_\mathrm{m} = E_\mathrm{i}\left(\frac{M}{m+M}\right)^2 = \eta_2^2 E_\mathrm{i}. \tag{1.12}$$

Substituting into Eq. (1.10b) and simplifying gives:

$$T = \frac{\gamma}{2} E_\mathrm{i}(1 - \cos\phi), \tag{1.13}$$

where we define

$$\gamma = \frac{4mM}{(M+m)^2} = \frac{4A}{(1+A)^2}, \tag{1.14}$$

where $1 = m$ and $A = M$. Hence, T depends upon only one unknown, ϕ. Note the angular dependence of T on ϕ as shown in Fig. 1.2. The energy transferred rises from 0 at $\phi = 0$ to a maximum of γE_i at $\phi = \pi$, or $T_\mathrm{max} = \hat{T} = \gamma E_\mathrm{i}$. That is, the energy transferred is a maximum when the particle backscatters and is a minimum when it misses the target, resulting in no change in course ($\phi = 0$).

Example 1.1. Neutron–nuclear interaction

For a neutron incident on a hydrogen atom, $\hat{T}_{n-H}/E_\mathrm{i} = 1.0$. For a neutron incident on a uranium atom, $\hat{T}_{n-U}/E_\mathrm{i} = 0.017$. Conversely, comparing the interaction of an iron atom with 100 keV Xe^+ ions or electrons, the value of γ for

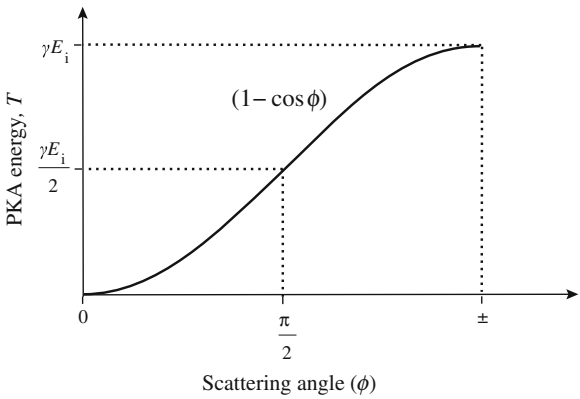

Fig. 1.2 Energy transfer as a function of center-of-mass scattering angle

the Xe–Fe interaction is 0.83, yielding a $\hat{T}$ of 83,000 eV. However, the value of γ for e^-–Fe interaction is 0.00004, giving a $\hat{T}$ of only 4 eV, which, as we will see in Chap. 2, is not enough to displace an iron atom from its lattice site.

The scattering angles in the laboratory system for the incident particle (θ) and the struck atom (α) can be written in terms of the scattering angle in the center-of-mass system (ϕ) using the vector diagram shown in Fig. 1.1(b). Applying the law of sines to Fig. 1.1(b) for the *scattered particle*:

$$\frac{v'_\ell}{\sin(\pi-\theta)} = \frac{v'_c}{\sin\theta},$$

where v'_c is given by Eqs. (1.6) and (1.7):

$$v'_c = V_{CM}\left(\frac{v_\ell}{V_{CM}} - 1\right),$$

and using Eq. (1.8), we have:

$$v'_c = V_{CM}\frac{M}{m}.$$

Applying the law of cosines to the same triangle gives:

$$v'^2_\ell = v'^2_c + V^2_{CM} - 2V_{CM}v'_c\cos(\pi-\phi),$$

and combining the last three equations to express θ as a function of ϕ yields:

$$\tan\theta = \frac{(M/m)\sin\phi}{1+(M/m)\cos\phi}.$$

Applying the law of sines to the vector diagram in Fig. 1.1(b) for the *struck atom* gives:

$$\frac{V_c'}{\sin\alpha} = \frac{V_\ell'}{\sin\phi},$$

and combining this result with Eqs. (1.6) and (1.9) where the energies are written in terms of velocities gives:

$$\tan\alpha = \frac{\sin\phi}{1-\cos\phi}.$$

We are still interested in obtaining the probability that a given T will be imparted to the recoil atom. This depends on the differential cross section. We define $\sigma_s(E_i, \phi)\,d\Omega$ as the probability of a collision that scatters the incident particle into a center-of-mass angle in the range $(\phi, d\Omega)$ where $d\Omega$ is an element of solid angle about the scattering direction ϕ. Since differential probabilities written in transformed variables are equivalent, $\sigma_s(E_i, \phi)$ can be written in terms of CM variables:

$$\sigma_s(E_i, \phi)d\Omega = \sigma_s(E_i, T)dT. \tag{1.15}$$

Using Fig. 1.3 to relate $d\Omega$ to $d\phi$, we have by definition:

$$d\Omega = dA/r^2, \tag{1.16}$$

and from Fig. 1.4, we have:

$$d\Omega = \frac{rd\phi(2\pi r\sin\phi)}{r^2} = 2\pi\sin\phi\,d\phi. \tag{1.17}$$

Substituting Eq. (1.17) into Eq. (1.15) yields:

$$\sigma_s(E_i, T)\,dT = \sigma_s(E_i, \phi)\,d\Omega = 2\pi\sigma_s(E_i, \phi)\sin\phi\,d\phi. \tag{1.18}$$

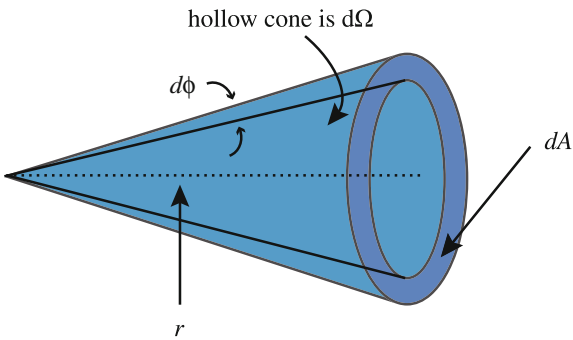

Fig. 1.3 Scattering into the solid angular element $d\Omega$ defined by dA/r^2

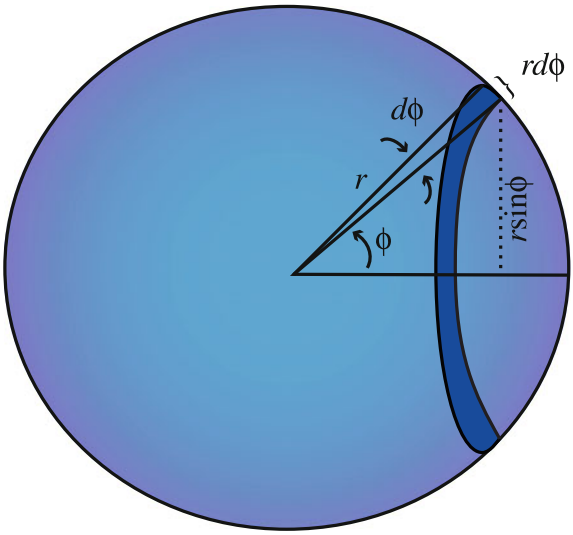

Fig. 1.4 The solid angle dΩ subtended at the scattering angle ϕ by the incremental angle dϕ

Since $T = \frac{\gamma}{2} E_\mathrm{i}(1 - \cos\phi)$ then $\mathrm{d}T = \frac{\gamma}{2} E_\mathrm{i} \sin\phi \, \mathrm{d}\phi$, and we have:

$$\sigma_\mathrm{s}(E_\mathrm{i}, T) = \frac{4\pi}{\gamma E_\mathrm{i}} \sigma_\mathrm{s}(E_\mathrm{i}, \phi). \tag{1.19}$$

Figure 1.5 shows the difference in the differential scattering cross section in units of area per unit solid angle versus area per unit angle as in Eq. (1.18). Although the number of atoms scattered through an angle increment dϕ about $\phi = \pi/2$ is greater than that through an angular increment dϕ about $\phi = 0$ or π (Fig. 1.5(a)), the number intercepting the spherical surface per unit of solid angle is constant over all angles, ϕ (Fig. 1.5(b)). Hence, dT/dϕ varies in a sinusoidal manner with ϕ, but dT/dΩ is independent of ϕ.

Using Eqs. (1.2) and (1.18), the total elastic scattering cross section is as follows:

$$\sigma_\mathrm{s}(E_\mathrm{i}) = \int \sigma_\mathrm{s}(E_\mathrm{i}, \phi) \, \mathrm{d}\Omega = 2\pi \int \sigma_\mathrm{s}(E_\mathrm{i}, \phi) \, \sin\phi \, \mathrm{d}\phi.$$

If we assume that elastic scattering in the CM system is independent of scattering angle (i.e., scattering is isotropic), Fig. 1.6, then:

$$\sigma_\mathrm{s}(E_\mathrm{i}) = \int \sigma_\mathrm{s}(E_\mathrm{i}, \phi) \, \mathrm{d}\Omega = 2\pi \, \sigma_\mathrm{s}(E_\mathrm{i}, \phi) \int \sin\phi \, \mathrm{d}\phi = 4\pi \, \sigma_\mathrm{s}(E_\mathrm{i}, \phi), \tag{1.20}$$

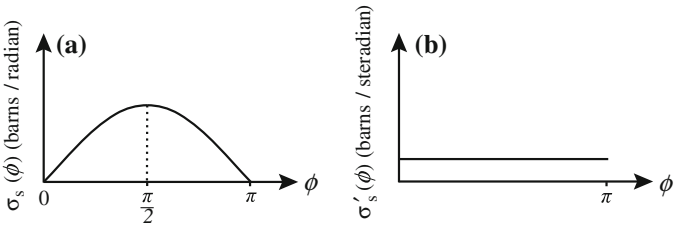

Fig. 1.5 Isotropic differential scattering cross sections in units of (**a**) area per unit scattering angle and (**b**) area per unit solid angle

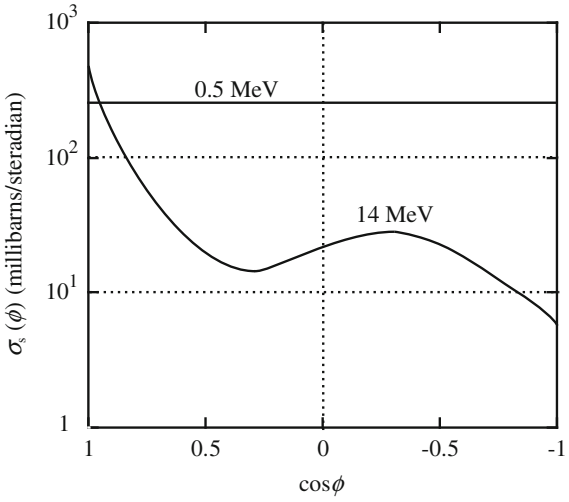

Fig. 1.6 Differential elastic scattering cross sections for C^{12} at 0.5 and 14 MeV neutrons as a function of the cosine of the center-of-mass scattering angle (from [2])

and

$$\sigma_s(E_i, T) = \frac{\sigma_s(E_i)}{\gamma E_i}, \tag{1.21}$$

which is independent of T! That is, σ_s (E_i, T), the probability that a neutron of energy E_i, elastically scattering against an atom of mass M, will impart a recoil energy T to the struck atom does not depend on the recoil energy. Now, the average recoil energy can be calculated as follows:

$$\overline{T} = \frac{\int_{\check{T}}^{\hat{T}} T\sigma_s(E_i, T)\,dT}{\int_{\check{T}}^{\hat{T}} \sigma_s(E_i, T)\,dT} = \frac{\check{T} + \hat{T}}{2} \approx \frac{\hat{T}}{2} = \frac{\gamma E_i}{2}. \tag{1.22}$$

Applying Eq. (1.22) to the case of a 1 MeV neutron incident on elements of varying mass, we have the following:

$$\begin{array}{lll} 1\,\text{MeV n on C:} & \gamma = 0.28 & \overline{T} = 0.14\,\text{MeV} \\ 1\,\text{MeV n on Fe:} & \gamma = 0.069 & \overline{T} = 0.035\,\text{MeV} \\ 1\,\text{MeV n on U:} & \gamma = 0.017 & \overline{T} = 0.009\,\text{MeV} \end{array}$$

In addition to the elastic scattering just discussed, we can have energy transfer by inelastic scattering, (n, 2n) reactions and (n, γ) reactions. The first two reactions become important above neutron energies of about 1.0 and 8.0 MeV, respectively, while the latter occurs at thermal neutron energies in ^{235}U.

1.1.2 Inelastic Scattering

Inelastic scattering is characterized by a reaction in which the emitted particle is experimentally the same as the captured particle, but there is a loss of kinetic energy in the system. The energy is found in the excitation energy of the product nucleus, e.g., N^{14} (p, p′)N^{14*} or C^{14}(n, n′)C^{14*}. The differences in the energies of groups of scattered particles correspond to the energy separations of excited levels in the product nucleus:

$$-Q = \sum_{\text{f}} KE_{\text{f}} - \sum_{\text{i}} KE_{\text{i}} = \sum_{\text{f}} M_{\text{f}}c^2 - \sum_{\text{i}} M_{\text{i}}c^2.$$

In an inelastic collision, a neutron is absorbed by the nucleus, forming a compound nucleus, which emits a neutron and a γ-ray. There may be more than one γ emitted and the nucleus may remain in an excited state during the course of an interaction. The inelastic scattering cross section can be divided into resolved and unresolved resonance components [3]. For a given resonance (jth resonance) of the target nucleus, the scattering cross section will be a function of Q_j, the γ decay energy of the residual nucleus that is always negative. Analogous to Eq. (1.15), we can write differential equalities σ_{sj} (E_{i}, Q_j, T) dT = σ_{sj} (E_{i}, Q_j, ϕ) dΩ, so that:

$$\sigma_{sj}(E_{\text{i}}, Q_j, T) = \sigma_{sj}(E_{\text{i}}, Q_j, \phi)\, 2\pi \sin\phi \frac{\text{d}\phi}{\text{d}T}. \tag{1.23}$$

However, the expression for T in Eq. (1.13) is not valid for inelastic collisions since kinetic energy is not conserved. Instead, we focus on the conservation of total energy. If the target nucleus M is at rest in the laboratory system and the particle m has energy E_{i}, then the energy balance in CM coordinates is as follows:

$$\frac{M}{M+m} E_{\text{i}} + Q_j = E'_{\text{m}} + E'_{\text{M}}, \tag{1.24}$$

where Q_j is the reaction energy and E'_{m} and E'_{M} are the kinetic energies in CM coordinates of the exit particle and nucleus, respectively. In order that momentum is conserved:

$$mE'_{\mathrm{m}} = ME'_{\mathrm{M}}, \tag{1.25}$$

and combining Eq. (1.24) with Eq. (1.25) (assuming that the masses of the projectile and target are unchanged after the reaction) yields:

$$E'_{\mathrm{m}} = \frac{M}{M+m}\left(Q_j + \frac{M}{M+m}E_{\mathrm{i}}\right)$$

or

$$E'_{\mathrm{m}} = \eta_2\left(Q_j + \eta_2 E_{\mathrm{i}}\right). \tag{1.26}$$

Recalling the general expression for T, Eq. (1.10b):

$$T = \eta_1\eta_2 E_{\mathrm{i}} + \frac{\eta_1}{\eta_2}E'_{\mathrm{m}} - 2\eta_1\left(E_{\mathrm{i}}E'_{\mathrm{m}}\right)^{1/2}\cos\phi,$$

and substituting in for E'_{m} from Eq. (1.26) yields:

$$T(E_{\mathrm{i}}, Q_j, \phi) = \frac{\gamma}{2}E_{\mathrm{i}} - \frac{\gamma}{2}\left[E_{\mathrm{i}}\left(E_{\mathrm{i}} + Q_j\frac{A+1}{A}\right)\right]^{1/2}\cos\phi + \frac{Q_j}{A+1}. \tag{1.27}$$

Now, the expression for $\mathrm{d}T/\mathrm{d}\phi$ becomes:

$$\frac{\mathrm{d}T(E_{\mathrm{i}}, Q_j, \phi)}{\mathrm{d}\phi} = \frac{\gamma}{2}E_{\mathrm{i}}\left[1 + \frac{Q_j}{E_{\mathrm{i}}}\frac{A+1}{A}\right]^{1/2}\sin\phi. \tag{1.28}$$

Note that in the case of elastic collisions, Q_j = 0 and Eq. (1.27) reduces to Eq. (1.13).

If we now assume that inelastic scattering is isotropic in the CM system, then we have:

$$\sigma_{\mathrm{s}j}(E_{\mathrm{i}}, Q_j) = \int \sigma_{\mathrm{s}j}(E_{\mathrm{i}}, Q_j, \phi)\,\mathrm{d}\Omega = 4\pi\sigma_{\mathrm{s}j}(E_{\mathrm{i}}, Q_j, \phi). \tag{1.29}$$

Substituting Eqs. (1.28) and (1.29) into (1.23) yields:

$$\sigma_{\mathrm{s}j}(E_{\mathrm{i}}, Q_j, T) = \frac{\sigma_{\mathrm{s}j}(E_{\mathrm{i}}, Q_j)}{\gamma E_{\mathrm{i}}\left(1 + \dfrac{Q_j}{E_{\mathrm{i}}}\dfrac{A+1}{A}\right)^{1/2}}. \tag{1.30}$$

for inelastic collisions in the resolved resonance region.

When the compound nucleus is excited to high enough energies, the resonance levels overlap and are no longer individually distinguishable. The inelastic scattering cross section is treated as a continuum and is described by an evaporation model [3] with:

$$\begin{aligned}\sigma_{\mathrm{is}}\left(E_{\mathrm{i}}, E'_{\mathrm{m}}, T\right) &= \sigma_{\mathrm{is}}\left(E_{\mathrm{i}}\right)\frac{f(E_{\mathrm{i}}, E'_{\mathrm{m}})}{4\dfrac{1}{A+1}\left(E_{\mathrm{i}}, E'_{\mathrm{m}}\right)^{1/2}}, \text{ and} \\ \sigma_{\mathrm{is}}\left(E_{\mathrm{i}}, T\right) &= \sigma_{\mathrm{is}}\left(E_{\mathrm{i}}\right)\int_0^{E'^{\max}_{\mathrm{m}}}\frac{f(E_{\mathrm{i}}, E'_{\mathrm{m}})}{4\dfrac{1}{A+1}\left(E_{\mathrm{i}}, E'_{\mathrm{m}}\right)^{1/2}}\mathrm{d}E'_{\mathrm{m}},\end{aligned} \tag{1.31}$$

where $f(E_{\mathrm{i}}, E'_{\mathrm{m}})$ is a distribution function for the energy E'_{m} of the scattered neutron in the CM system that represents the probability that a neutron is evaporated from the moving compound nucleus, whose value in the CM system is a Maxwellian of nuclear temperature $E_{\mathrm{D}} = kT$:

$$f(E_{\mathrm{i}}, E'_{\mathrm{m}}) = \frac{E'_{\mathrm{m}}}{I(E_{\mathrm{i}})}\mathrm{e}^{(-E'_{\mathrm{m}}/E_{\mathrm{D}})}, \tag{1.32}$$

and

$$I(E_{\mathrm{i}}) = E_{\mathrm{D}}^2\left[1 - \left(1 + \frac{E'^{\max}_{\mathrm{m}}}{E_{\mathrm{D}}}\right)\mathrm{e}^{(-E'^{\max}_{\mathrm{m}}/E_{\mathrm{D}})}\right], \tag{1.33}$$

is a normalization factor such that

$$\int_0^{E'^{\max}_{\mathrm{m}}} f(E_{\mathrm{i}}, E'_{\mathrm{m}})\,\mathrm{d}E'_{\mathrm{m}} = 1. \tag{1.34}$$

The maximum value of E'_{m} is given by Eq. (1.26) with $Q = Q_1$, the lowest energy level, and the minimum value of E'_{m} is zero.

1.1.3 (n, 2n) Reactions

Reactions such as the (n, 2n) reaction are important in radiation effects since they produce additional neutrons that can either cause damage or transmutation reactions in components of interest. Following the 2n model, which is based on work by Odette [4] and Segev [5], a second neutron can only be emitted if the residual excitation of the nucleus after emission of the first neutron exceeds the binding energy of a neutron in the mass M nuclide. The recoil energy after emission of the

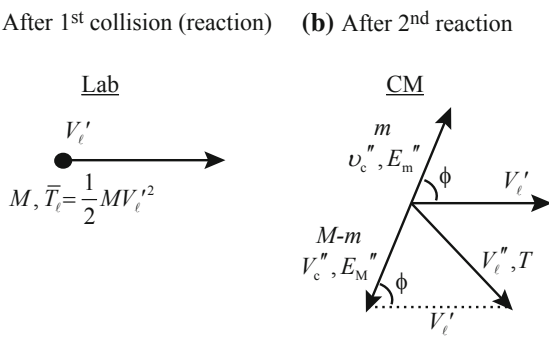

Fig. 1.7 Vector velocities for the (n, 2n) reaction in (**a**) the laboratory system and (**b**) the center-of-mass system

first neutron is taken to be the average value ($\cos\phi = 0$ in Eq. (1.10b)) and is shown in Fig. 1.7(a) in the laboratory system. We next analyze the second reaction (emission) in the CM system described in Fig. 1.7(b). We begin by using the law of cosines to relate V_c'' to ϕ:

$$V_\ell''^2 = V_\ell'^2 + V_c''^2 - 2V_\ell' V_c'' \cos\phi. \tag{1.35}$$

From Fig. 1.7(a), we have:

$$\frac{1}{2}MV_\ell'^2 = \overline{T}_\ell \quad \text{or} \quad V_\ell'^2 = \frac{2\overline{T}_\ell}{M},$$

and from Fig. 1.7(b), we have:

$$\frac{1}{2}(M-m)V_c''^2 = E_M'' \quad \text{or} \quad V_c''^2 = \frac{2E_M''}{M-m}.$$

Conservation of momentum requires:

$$(M-m)V_c'' = m\upsilon_c'', \tag{1.36}$$

and squaring gives:

$$V_c''^2 = \left(\frac{m}{M-m}\right)^2 \upsilon_c''^2 = \frac{2m}{(M-m)}E_m''. \tag{1.37}$$

Substituting into the law of cosines, Eq. (1.35), gives:

$$V_\ell''^2 = \frac{2\overline{T}_\ell}{M} + \frac{2m}{(M-m)}E_m'' - 2\left(\frac{2m}{(M-m)^2}\frac{2}{M}E_m''\overline{T}_\ell\right)^{1/2}\cos\phi, \tag{1.38}$$

where $\overline{T}_\ell = \eta_1\eta_2 E_\mathrm{i} + (\eta_1/\eta_2)E'_\mathrm{m}$ is the mean recoil energy after the emission of the first neutron. Writing V''^2_ℓ in terms of energy gives the recoil energy following the second emission:

$$\begin{aligned} T &= \frac{1}{2}(M-m)V''^2_\ell \\ &= \frac{M-m}{M}\overline{T}_\ell + \frac{m}{M-m}E''_\mathrm{m} - 2\left(\frac{m}{M}\right)^{1/2}(E''_\mathrm{m}\overline{T}_\ell)^{1/2}\cos\phi \\ &= \frac{A-1}{A}\overline{T}_\ell + \frac{1}{A-1}E''_\mathrm{m} - 2\left(\frac{1}{A}\right)^{1/2}(\overline{T}_\ell E''_\mathrm{m})^{1/2}\cos\phi \\ &= \frac{A}{A-1}\frac{\eta_1}{\eta_2}E''_\mathrm{m} + \frac{A-1}{A}\overline{T}_\ell - 2\left(\frac{\eta_1}{\eta_2}\right)^{1/2}(\overline{T}_\ell E''_\mathrm{m})^{1/2}\cos\phi. \end{aligned} \tag{1.39}$$

The (n, 2n) reaction cross section is a special case of the inelastic scattering cross section given in Eq. (1.31):

$$\begin{aligned} &\sigma_{\mathrm{n,2n}}(E_\mathrm{i}, E'_\mathrm{m}, E''_\mathrm{m}, T) \\ &\quad = \sigma_{\mathrm{n,2n}}(E_\mathrm{i})\frac{E'_\mathrm{m}}{I(E_\mathrm{i})}\mathrm{e}^{-E'_\mathrm{m}/E_\mathrm{D}}\frac{E''_\mathrm{m}}{I(E_\mathrm{i}, E'_\mathrm{m})}\mathrm{e}^{-E''_\mathrm{m}/E_\mathrm{D}}, \quad \text{and} \\ &\sigma_{\mathrm{n,2n}}(E_\mathrm{i}, T) \\ &\quad = \int_0^{E_\mathrm{i}-U}\frac{E'_\mathrm{m}}{I(E_\mathrm{i})}\mathrm{e}^{-E'_\mathrm{m}/E_\mathrm{D}}\int_0^{E_\mathrm{i}-U-E'_\mathrm{m}}\frac{E''_\mathrm{m}}{I(E_\mathrm{i}, E'_\mathrm{m})}\mathrm{e}^{-E''_\mathrm{m}/E_\mathrm{D}}\mathrm{d}E'_\mathrm{m}\mathrm{d}E''_\mathrm{m}, \end{aligned} \tag{1.40}$$

where $I(E_\mathrm{i})$ is given in Eq. (1.33) with $E'^{\max}_\mathrm{m} = E_\mathrm{i} - U$ and $I(E_\mathrm{i}, E'_\mathrm{m})$ is given in Eq. (1.33) with $E'^{\max}_\mathrm{m}$ replaced by $E''^{\max}_\mathrm{m} = E_\mathrm{i} - U - E'_\mathrm{m}$ and for (n, 2n) reactions, $U = 0$ [3].

1.1.4 (n, γ) Reactions

Another class of reactions that can affect the extent of radiation damage involves photon emission. This reaction is important since the energy of the recoiling nucleus is sufficient to displace an atom. As we will see later, this type of displacement is particularly important in radiation damage in reactor pressure vessels in which the gamma flux is more comparable to the fast neutron flux than in the reactor core. Recalling the momentum and energy conservation laws of Eqs. (1.3) and (1.4) and Fig. 1.1, which for (n, γ) reactions, $E_\mathrm{i} \sim 0$ (since these reactions occur with thermal neutrons of energy 0.025 eV), $E_\mathrm{f} \equiv 0$ (since there is no scattered neutron) and Q is the equivalent of the mass difference between the initial particles and the compound nucleus. When the compound nucleus (CN) de-excites, it emits a

γ-ray with this energy. Conservation of momentum says that the nucleus must recoil with momentum:

$$(m+M)V_c' = \frac{E_\gamma}{c}. \tag{1.41}$$

Note that this is an approximation since we have not subtracted the mass defect from the compound nucleus. Squaring both sides of Eq. (1.41) and dividing by 2 (m + M) gives:

$$\frac{1}{2}(m+M)V_c'^2 = \frac{E_\gamma^2}{2(m+M)c^2}.$$

As in the case of elastic scattering, T is given by:

$$T = (V_{CM}^2 + V_c'^2 - 2V_{CM}V_c'\cos\phi)\left(\frac{M+m}{2}\right),$$

but $V_{CM} \ll V_c'$ so to a good estimate:

$$T \cong \left(\frac{m+M}{2}\right)V_c'^2 = \frac{E_\gamma^2}{2(M+m)c^2}.$$

We will assume further that this value of T represents the maximum recoil energy. But since not all of Q will be emitted in a single γ-ray, we approximate the average recoil energy as half the value of the maximum recoil energy, giving:

$$\overline{T} \cong \frac{E_\gamma^2}{4(M+m)c^2}. \tag{1.42}$$

The radiative capture cross section is derived from the Breit–Wigner single-level formula when the target nucleus has zero intrinsic angular momentum and the compound nucleus has a neutron width Γ_n, a radiation width Γ_g, and a total width Γ, and E_0 is the resonance energy and λ is the wavelength [6]:

$$\sigma_{n,\gamma}(E_i) = \pi\lambda^2 \frac{\Gamma_n\Gamma_\gamma}{(E_i - E_0)^2 + (\Gamma/2)^2}. \tag{1.43}$$

Expressing Eq. (1.43) in terms of σ_0, the maximum value of the radiative capture cross section (at $E = E_0$) and taking Γ_n proportional to $1/\lambda$ and to $\sqrt{E}$ gives:

$$\sigma_{n,\gamma}(E_i) = \sigma_0\sqrt{\frac{E_0}{E_i}}\left\{\frac{1}{[(E_i - E_0)/(\Gamma/2)]^2 + 1}\right\}. \tag{1.44}$$

Table 1.2 Energy transfer and energy transfer cross sections for various types of neutron–nuclear collisions

Types of collision	Energy transfer and energy transfer cross section	Equation in text
Elastic scattering	$T = \frac{\gamma}{2} E_\mathrm{i}(1 - \cos\phi)$	(1.13)
	$\sigma_\mathrm{s}(E_\mathrm{i}, T) = \frac{\sigma_\mathrm{s}(E_\mathrm{i})}{\gamma E_\mathrm{i}}$	(1.21)
Inelastic scattering	$T(E_\mathrm{i}, Q_j, \phi) = \frac{\gamma}{2} E_\mathrm{i} - \frac{\gamma}{2}\left[E_\mathrm{i}\left(E_\mathrm{i} + Q_\mathrm{i}\frac{A+1}{A}\right)\right]^{1/2} \cos\phi + \frac{Q_j}{A+1}$	(1.27)
	resonance region	
	$\sigma_{\mathrm{s},j}(E_\mathrm{i}, Q_j, T) = \frac{\sigma_{\mathrm{s},j}(E_\mathrm{i}, Q_j)}{\gamma E_\mathrm{i}\left(1 + \frac{Q_j}{E_\mathrm{i}}\frac{1+A}{A}\right)^{1/2}}$	(1.30)
	unresolved resonance region	
	$\sigma_\mathrm{is}(E_\mathrm{i}, T) = \sigma_\mathrm{is}(E_\mathrm{i}) \int_0^{E_\mathrm{m}^\mathrm{max}} \frac{f(E_\mathrm{i}, E'_\mathrm{m})}{4\frac{1}{A+1}(E_\mathrm{i}, E'_\mathrm{m})^{1/2}}\, \mathrm{d}E'_\mathrm{m}$	(1.31)
(n, 2n)	$T = \frac{A}{A-1}\frac{\eta_1}{\eta_2} E''_\mathrm{m} + \frac{A-1}{A}\overline{T}_\ell - 2\left(\frac{\eta_1}{\eta_2}\right)^{1/2} (\overline{T}_\ell E''_\mathrm{m})^{1/2} \cos\phi$	(1.39)
	$\sigma_{\mathrm{n,2n}}(E_\mathrm{i}, T) = \int_0^{E_\mathrm{i}-U} \frac{E'_\mathrm{m}}{I(E_\mathrm{i})} \mathrm{e}^{-E'_\mathrm{m}/E_\mathrm{D}} \times \int_0^{E_\mathrm{i}-U-E'_\mathrm{m}} \frac{E''_\mathrm{m}}{I(E_\mathrm{i}, E'_\mathrm{m})} \mathrm{e}^{-E''_\mathrm{m}/E_\mathrm{D}} \mathrm{d}E'_\mathrm{m}\, \mathrm{d}E''_\mathrm{m}$	(1.40)
(n, γ)	$\overline{T} \cong \frac{E_\gamma^2}{4(M+m)c^2}$	(1.42)
	$\sigma_{\mathrm{n},\gamma}(E_\mathrm{i}) = \sigma_0 \sqrt{\frac{E_0}{E_\mathrm{i}}} \left\{ \frac{1}{[(E_\mathrm{i} - E_0)/(\Gamma/2)]^2 + 1} \right\}$	(1.44)

Table 1.2 provides a summary of the energy transfer and the energy transfer cross sections for the various types of reactions covered in Sect. 1.1.

1.2 Interactions Between Ions and Atoms

Ion–atom or atom–atom collisions are governed by interactions between the electron clouds, the electron cloud and the nucleus, and between the nuclei. These interactions are described by what are known as interatomic potentials. In order to develop descriptions of energy transfer cross sections for interactions between atoms, we need descriptions of the potential function that governs that interaction. Unfortunately, there exists no single function that describes all interactions, but rather, the nature of the interaction is a strong function of the atom energies, and hence the distance of closest approach of the nuclei. The following section provides a summary of interatomic potentials adapted from Chadderton [7].

1.2.1 Interatomic Potentials

The end product of the neutron–nuclear interaction is the creation of the primary knock-on atom with some amount of kinetic energy. This atom will, of course, make subsequent collisions with other atoms in the solid. Knowledge of the forces acting between two colliding atoms represents the most fundamental aspect of radiation damage, without which a proper description of the primary event and the ensuing defect structure is impossible. Our interest lies in the forces between like atoms, unlike atoms, or ions and atoms. The interaction between atoms is described by potential functions. Recall that the atoms are (usually) electrically neutral but are composed of positive and negative components that do not cancel at all points in space. It is well known that the potential energy between two point charges of the same sign separated by a distance r is described by the well-known Coulomb equation:

$$V(r) = k_e \frac{\varepsilon^2}{r}, \tag{1.45}$$

where $k_e = \dfrac{1}{4\pi\varepsilon_0}$ is the Coulomb constant (8.98755×10^9 Nm^2 C^{-2}), ε_0 is the electric constant, ε is the single unit electronic charge, and ε^2 = 1.44 eV-nm. When written in electrostatic units or Gaussian units, the unit charge (esu or statcoulomb) is defined in such a way that the Coulomb constant, k_e, disappears because it has the value of one and becomes dimensionless, and Eq. (1.45) is often written in abbreviated form without the Coulomb constant. In the case of atoms, we have a charged nucleus surrounded by an electron cloud of opposite charge. It is evident that the potential function describing the interaction between atoms is far more complicated than that describing neutron–nuclear interaction. Even in the simplest cases, $V(r)$ has never been determined exactly, but some simple considerations show that it must be dominated by two distinct contributions over the range of separation in which we are interested. Perhaps, the simplest of all potential functions is the "hard sphere" approximation. This potential is described as follows:

$$V(r) = \begin{cases} 0 & \text{for } r > r_0 \\ \infty & \text{for } r \leq r_0. \end{cases} \tag{1.46}$$

This potential function describes an interaction with an infinitely sharp cutoff at the atomic radius r_0. At distances greater than this radius, the interaction vanishes, while at distances equal to and less than r_0, the magnitude is infinity. This description is analogous to the behavior of billiard balls, and hence, the atoms in this model are described as acting as such. Clearly, this is not a very realistic description of atom–atom interaction since we know that the electron shells can overlap.

Figure 1.8 shows how the interatomic potential actually varies with separation. At large separation, the principal interaction is supplied by the Coulomb forces,

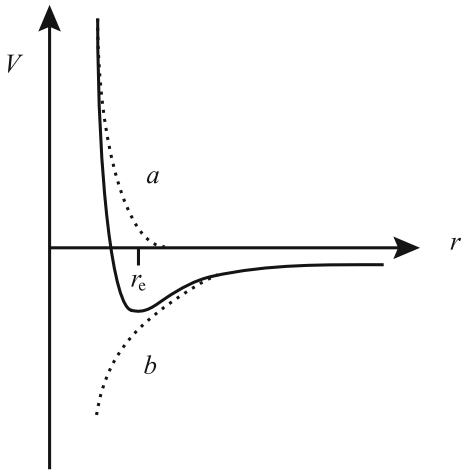

Fig. 1.8 Variation of interatomic potential with separation, *R*. Attractive forces dominate at large separations (*b*) and the central repulsive force dominates at small separations, (*a*) and at intermediate distances, there is a smooth transition between the two extremes with a minimum corresponding to the equilibrium separation distance, r_e or *D*

while for smaller separations, the central field repulsive force is dominant. A similar relationship applies to all crystals regardless of the nature of binding. In all cases, there is a smooth curve with a minimum at the separation distance corresponding to the nearest neighbor distance in the lattice, r_e (also referred to as *D*).

In describing the interaction between atoms, we will use two yardsticks for points of reference. One is the Bohr radius of the hydrogen atom, $a_0 = 0.053$ nm, which provides a measure of the position of the atomic shells. The other is r_e, the spacing between nearest neighbors in the crystal (typically ~ 0.25 nm). When $r \ll r_e$, electrons populate the lowest energy levels (closed shells) of the individual atoms and only the outer valence shells will have empty levels. As two atoms are brought together, the valence shells begin to overlap and weak attractive forces such as van der Waals forces may develop. When $a_0 < r \leq r_e$, the closed inner shells begin to overlap. Since the Pauli exclusion principle demands that some electrons change their levels, and hence move to higher energy levels, the extra energy supplied in forcing the atoms together constitutes a positive potential energy of interaction. This is known as closed shell repulsion and the potential that most accurately describes this region is the Born–Mayer potential:

$$V(r) = A \exp(-r/B), \tag{1.47}$$

where *A* and *B* are constants determined from the elastic moduli [8]. Although this function was first used by Born and Mayer to represent core ion repulsion in their theory of ionic crystals, it is perfectly valid for separations on the order of the

equilibrium separation, r_e, and is useful in treatments of threshold or near-threshold collisions where the impact parameter is of the order r_e.

When $r \ll a_0$, Coulomb interaction between the nuclei dominates all other terms in $V(r)$:

$$V(r) = \frac{Z_1 Z_2 \varepsilon^2}{r}. \tag{1.48}$$

At slightly larger distances, the nuclear charges are electrostatically "screened" by the space charge of the innermost electron shells that have entered the internuclear space. The potential describing this behavior is known as the screened Coulomb potential [8–12]:

$$V(r) = \left(\frac{Z_1 Z_2 \varepsilon^2}{r}\right) \exp(-r/a), \tag{1.49}$$

where $a = \left(\frac{9\pi^2}{128}\right)^{1/3} \frac{a_0}{(Z_1^{2/3} + Z_2^{2/3})^{1/2}} \approx \frac{Ca_0}{(Z_1 Z_2)^{1/6}}$ is the screening radius and $C = 0.8853$. More generally, screening by the electron cloud is described by a screening function, $\chi(r)$, that is defined as the ratio of the actual atomic potential at a radius r to the Coulomb potential. The function of $\chi(r)$ is to moderate the Coulomb potential to describe the interaction between atoms at all separation distances. For large distances, $\chi(r)$ will tend toward zero, and at very small distances, $\chi(r)$ will tend toward unity. This is one way in which a single interatomic potential function can be used to describe all collisions.

We have now described two regimes of interaction. At small separations ($r < a$), the screened Coulomb term dominates all others, with the screening effect decaying exponentially with the separation distance. In the region $r \lesssim r_e$, electronic interaction dominates and is best described by the Born–Mayer potential. At intermediate separations, there is no satisfactory description of the nature of atomic interaction. Unfortunately, it is exactly in this region where information is needed to provide a proper analytical description of radiation damage.

Nevertheless, we may make a first approximation to the total potential by summing the controlling potentials at large and small separations:

$$V(r) = \left(\frac{Z_1 Z_2 \varepsilon^2}{r}\right) \exp(-r/a) + A \exp(-r/B), \tag{1.50}$$

where $A = 2.58 \times 10^{-5} (Z_1 Z_2)^{11/4}$ eV and $B = 1.5 a_0/(Z_1 Z_2)^{1/6}$ are empirical formulae suggested by Brinkman [11], consistent with observed compressibilities and elastic moduli in the noble metals Cu, Ag, and Au. Unfortunately, there is little experimental information about the forces between metal atoms, which is our primary interest. Figure 1.9 shows that the first term dominates for small separation and the second for large.

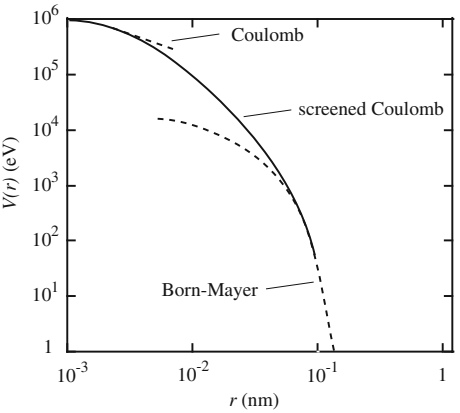

Fig. 1.9 Behavior of various potential functions over a range of separation distances between copper atoms

Brinkman suggested a model for the interaction between two identical atoms in which the nucleus is surrounded by a rigid charge distribution ρ_ε, and it is assumed that both atoms supply a screened Coulomb field of the same type:

$$V(r) = \frac{Z^2\varepsilon^2}{r} e^{-r/a}\left(1 - \frac{r}{2a}\right). \tag{1.51}$$

This relation approaches the Coulomb repulsion as r approaches zero and changes sign at $r = 2a$, becoming a weak attractive potential with a minimum at $r = a(1 + \sqrt{3})$. However, this potential predicts a strong interaction energy at large distances and may not represent the true physical picture for metals. Brinkman formulated a new potential function:

$$V(r) = \frac{AZ_1Z_2\varepsilon^2 \exp(-Br)}{1 - \exp(-Ar)}. \tag{1.52}$$

Note that for small values of r, the potential closely approximates the Coulomb repulsive interaction, i.e.,

$$\lim_{r\to 0} V(r) \to \frac{Z_1Z_2\varepsilon^2}{r},$$

and at large separation, the potential equation approximates the exponential repulsion of the Born–Mayer type:

$$\lim_{r\to\infty} V(r) \to AZ_1Z_2\varepsilon^2 \exp(-Br).$$

The constant B is defined as $B = Z_{\text{eff}}^{1/3}/Ca_0$, where $Z_{\text{eff}} = (Z_1Z_2)^{1/2}$, and C is of the order 1.0 or 1.5. The constant A depends on the compressibility and bulk modulus, which depend on the overlap of closed electron shells. An empirical

expression for A is $A = \dfrac{0.95 \times 10^{-6}}{a_0} Z_{\text{eff}}^{7/6}$ Substituting for A, B, and C (= 1.5) into Eq. (1.52) gives:

$$V(r) = 1.9 \times 10^{-6} Z_{\text{eff}}^{1/2} E_{\text{R}} \frac{\exp\left(-Z_{\text{eff}}^{1/3} r / 1.5 a_0\right)}{1 - \exp\left(-0.95 \times 10^{-6} Z_{\text{eff}}^{7/6} r / a_0\right)}, \tag{1.53}$$

where $E_{\text{R}} = \varepsilon^2/2a_0$ is the Rydberg energy (13.6 eV).

It should be noted that although the potential is a reasonably reliable function for all metals whose atomic number exceeds 25 over the range $r < 0.7 r_{\text{e}}$, it should not be used near $r = r_{\text{e}}$ since in the derivation it has been implicitly assumed that all interatomic distances are close to those of Cu, Ag, and Au. It is therefore not a valid potential to use in calculating formation and migration energies of point defects.

Two other potentials should be discussed. The first is the Firsov or Thomas–Fermi two-center potential. This potential function is an improvement over the screened Coulomb potential by virtue of the fact it takes into account the change in electron energy connected with the mutual approach of the nuclei. The potential can be written as follows:

$$V(r) = \frac{\chi(r)}{r},$$

where $\chi(r)$ is the screening function. In the case of the screened Coulomb potential:

$$\begin{aligned} \chi(r) &= \chi_{\text{B}}(r) \quad \text{and} \\ \chi_{\text{B}}(r) &= Z_1 Z_2 \varepsilon^2 \exp(-r/a), \end{aligned} \tag{1.54}$$

while in the Firsov potential:

$$\chi(r) = \chi_{\text{TF}}(r) = \chi\left[\left(Z_1^{1/2} + Z_2^{1/2}\right)^{2/3} \frac{r}{a}\right], \tag{1.55}$$

so that we have:

$$V(r) = \frac{Z_1 Z_2 \varepsilon^2}{r} \chi\left[\left(Z_1^{1/2} + Z_2^{1/2}\right)^{2/3} \frac{r}{a}\right], \tag{1.56}$$

where

$$\chi\left[\left(Z_1^{1/2} + Z_2^{1/2}\right)^{2/3} \frac{r}{a}\right]$$

is a screening function.

The second potential of interest is the Thomas–Fermi–Dirac two-center potential (TFD). The Thomas–Fermi–Dirac statistical model of the atom was employed to calculate a potential from first principles. As a consequence, this potential takes into account the exchange effects and places a finite boundary, defined by r_b, on the spatial distribution of the electron cloud density ρ_ε. The potential obtained for like atoms is as follows:

$$\overline{V}(r) = \frac{Z^2\varepsilon^2}{r}\chi\left(Z^{1/3}\frac{r}{a}\right) - \alpha Z + \overline{\Lambda}\,, \tag{1.57}$$

where $\alpha \cong 3.16 \times 10^{-3}\dfrac{\varepsilon^2}{a_0}$ and $\overline{\Lambda}$ is a set of integrals over exact single-center electron densities. Calculations using this potential have shown that for very small separations of less than $\sim 0.3a_0$, $\overline{V}(r)$ agrees well with other theoretical curves and with experiment, while in the range $\sim 0.3a_0$ to $3a_0$, $V(r)$ agrees with other theoretical and experiment results better than the screened Coulomb potential or the Firsov potential [7].

In selecting the appropriate potential for a specific collision problem, the range of separation can be determined by equating the available kinetic energy to the potential and hence obtaining the smallest separation. The important interaction terms for the calculated separation can then be determined. For interactions between metal atoms at low kinetic energies, 10^{-1} to 10^3 eV, the Born–Mayer term alone is sufficient with constants given in Eq. (1.50). In cases of atom–atom collisions in the collision cascade, where energies from 10^3 to 10^5 eV are involved, an inverse power potential is extremely convenient. Such a potential can be formulated by fitting a function C/r^s to one of the above potential functions over a limited range of r. For example, one can fit an inverse square ($s = 2$) function to the screened Coulomb potential at $r = a$, obtaining the same slope, ordinate, and curvature. This function is as follows[13]:

$$V(r) = \frac{Z_1 Z_2 \varepsilon^2 a}{r^2} e^{-1}. \tag{1.58}$$

For a limited range of r, this can be used as an approximate potential. Rewriting using the expression in Eq. (1.49) for a gives:

$$V(r) = \frac{2E_R}{e}(Z_1Z_2)^{5/6}\left(\frac{a_0}{r}\right)^2. \tag{1.59}$$

A convenient alternative for numerical calculations uses the fact that $\dfrac{2E_R}{e} \cong 10\,\text{eV}$, hence:

$$V(r) = 10(Z_1Z_2)^{5/6}\left(\frac{a_0}{r}\right)^2 \text{eV}. \tag{1.60}$$

Table 1.3 Summary of potential functions

Potential	Equation for $V(r)$ =	Range of applicability	Definitions	Eq. in text
Hard sphere	0 for $r > r_0$ ∞ for $r \leq r_0$	$10^{-1} < T < 10^3$ eV	r_0 = Atomic radius	(1.46)
Born–Mayer	$V(r) = A\exp(-r/B)$	$10^{-1} < T < 10^3$ eV $r \lesssim r_e$	A, B determined from elastic moduli	(1.47)
Simple Coulomb	$\frac{Z_1 Z_2 \varepsilon^2}{r}$	Light ions of high energy $r \ll a_0$		(1.48)
Screened Coulomb	$\left(\frac{Z_1 Z_2 \varepsilon^2}{r}\right) \exp(-r/a)$	Light ions $r < a$	a_0 = Bohr radius a = Screening radius	(1.49)
Brinkman I	$\frac{Z^2 \varepsilon^2}{r} e^{(-r/a)} \left(1 - \frac{r}{2a}\right)$	$r < a$	$a \cong a_0 / Z^{1/3}$	(1.51)
Brinkman II	$\frac{A Z_1 Z_2 \varepsilon^2 \exp(-Br)}{1 - \exp(-Ar)}$	Z > 25 $r < 0.7 r_e$	$A = \frac{0.95 \times 10^{-6}}{a_0} Z_{\text{eff}}^{7/6}$ $B = Z_{\text{eff}}^{1/3} / C a_0$ $C \cong 1.5$	(1.52)
Firsov	$\frac{Z_1 Z_2 \varepsilon^2}{r} \chi\left[\left(Z_1^{1/2} + Z_2^{1/2}\right)^{2/3} \frac{r}{a}\right]$	$r \leq a_0$	χ is screening function	(1.56)
TFD two-center	$\frac{Z^2 \varepsilon^2}{r} \chi\left(Z^{1/3} \frac{r}{a}\right) - \alpha Z + \overline{A}$	$r < r_b(3a_0)$	r_b = Radius at which the electron cloud density vanishes	(1.57)
Inverse square	$\frac{2E_R}{e} (Z_1 Z_2)^{5/6} \left(\frac{a_0}{r}\right)^2$	$a/2 < r < 5a$	E_R = Rydberg energy = 13.6 eV	(1.59)

This potential also applies to heavy ion bombardment in the energy range 10^3 to 10^5 eV. In the case of light ions at high energy, such as 5 MeV protons, the simple Coulomb potential is adequate.

Table 1.3 summarizes the various potential functions and their regions of applicability. But how do we go about verifying a potential function? For example, how do we determine the constants A and B in the Born–Mayer potential for a specific element? Since the Born–Mayer potential is based on small displacements from equilibrium (i.e., r_e), we can obtain these constants from bulk property measurement of the solid, e.g., compressibility and elastic moduli. If we expand the potential $V(r)$ as $V_0 + \left(\frac{dV}{dr}\right)_0 r + 1/2 \left(\frac{d^2V}{dr^2}\right)_0 r^2 + \cdots$, then the coefficient of $\left(\frac{d^2V}{dr^2}\right)_0$ is the curvature of the energy–distance curve at $r = r_e$ as shown in Fig. 1.8.

How then do we know that a given potential does or does not properly describe the interaction in a region of r? We can make this determination by scattering measurements or by measuring the range of ions in solids. Since $V(r)$ describes the nature of the interaction, it will also tell us about $\sigma_s(E_i)$ that can be determined by scattering experiments. Also, range measurements give a good indication of how many interactions must have occurred in order to place the ion in its deposited

location. Both of these sets of experiments will provide information on the adequacy of the chosen potential function to accurately describe the interaction between the atoms in the solid.

With some appreciation for the way in which neutral atoms or atoms and ions interact, we are now prepared to describe a collision between these species, which is in some ways very similar to and in other ways very different from neutron–nuclear collisions. The resulting formalism will provide us with the tools to determine the energy transferred from the incident atom to the struck atom along with the energy transfer cross section. The following treatment is adapted from Thompson [13].

1.2.2 Collision Kinematics

The orbits of two colliding atoms are shown in Fig. 1.10 relative to the center of mass of the masses M_1 and M_2. Particle locations are most conveniently denoted in polar coordinates (r_1, ψ) and (r_2, ψ) for masses M_1 and M_2, respectively. The impact parameter is b, ψ is the scattering angle of the struck atom in the laboratory system, and ϕ is the asymptotic scattering angle when the interparticle spacing approaches infinity. The impact parameter is defined as the distance between the asymptotic trajectories of the colliding particles as shown in Fig. 1.10. We are interested in determining the detailed orbits by expressing ϕ as a function of b. This result will then be used to determine the scattering cross section.

The radial and transverse velocities of mass M_1 are $\dot{r}_1$ and $r_1\dot{\psi}$ in polar coordinates, and the resultant velocity is $\left(\dot{r}_1^2 + r_1^2\dot{\psi}^2\right)^{1/2}$. The velocity components are the same for mass M_2 with the subscript 2 substituted for 1. Conservation of energy requires that the total energy of any system remains constant. The energy in the laboratory reference

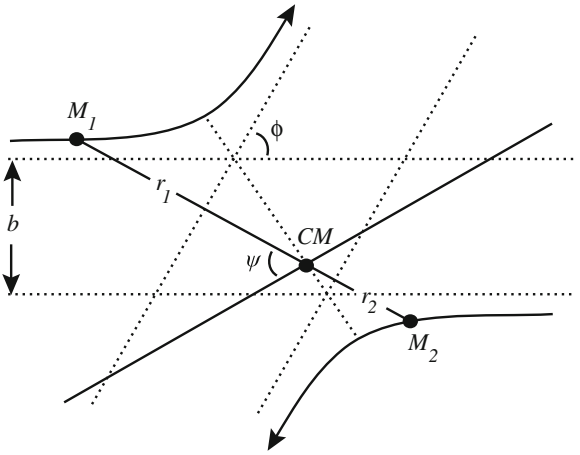

Fig. 1.10 Collision orbits in the center-of-mass system

system is just $E_i = \frac{1}{2}M_1 v_\ell^2 = E_T$ Recall that $V_{CM} = \frac{M_1}{M_1 + M_2} v_\ell$ and that the kinetic energy of the center of mass itself (in the laboratory system) is as follows:

$$E_{CM} = \frac{1}{2}(M_1 + M_2)V_{CM}^2 = \left(\frac{M_1}{M_1 + M_2}\right)E_i.$$

Hence, the energy in the CM system that is available for transformation is the total kinetic energy less the motion energy of the CM system:

$$E = E_T - E_{CM} = E_i - E_{CM} = E_i\left(\frac{M_2}{M_1 + M_2}\right). \tag{1.61}$$

In an elastic collision, the sum of the potential and kinetic energies at any point in the orbit must equal the asymptotic sum of kinetic energies, so:

$$E_i\left(\frac{M_2}{M_1 + M_2}\right) = \frac{1}{2}M_1(\dot{r}_1^2 + r_1^2\dot{\psi}^2) + \frac{1}{2}M_2(\dot{r}_2^2 + r_2^2\dot{\psi}^2) + V(r_1 + r_2). \tag{1.62}$$

asymptotic energy — sum of kinetic energy at any point in orbit — potential energy

Letting $r = r_1 + r_2$ be the total separation distance, $r_1 = \frac{M_2}{M_1 + M_2}r,\ r_2 = \frac{M_1}{M_1 + M_2}r$, and the energy balance of Eq. (1.62) simplifies to:

$$\eta E_i = \frac{1}{2}\mu(\dot{r}^2 + r^2\dot{\psi}^2) + V(r), \tag{1.63}$$

where $\eta = \frac{M_2}{M_1 + M_2}$ and $\mu = \frac{M_1 M_2}{M_1 + M_2}$ is the reduced mass.

The law of conservation of angular momentum demands that the value at any point in the orbit must equal the asymptotic value. Recall that:

$$v_\ell = v_\ell - V_{CM} = v_\ell\left(\frac{M_2}{M_1 + M_2}\right) \text{ and } V_2 = V_{CM} = v_\ell\left(\frac{M_1}{M_1 + M_2}\right),$$

so that the asymptotic value of the angular momentum is given by:

$$M_1 v_1 b_1 + M_2 v_2 b_2 = \left(\frac{M_1 M_2}{M_1 + M_2}\right) v_\ell(b_1 + b_2) = \mu b v_\ell. \tag{1.64}$$

The angular momentum at any point is given by:

$$\begin{aligned} M_1 r_1^2\dot{\psi} + M_2 r_2^2\dot{\psi} &= \left[M_1\left(\frac{M_2}{M_1 + M_2}r\right)^2 + M_2\left(\frac{M_1}{M_1 + M_2}r\right)^2\right]\dot{\psi} \\ &= \mu r^2\dot{\psi}, \end{aligned} \tag{1.65}$$

hence:

$$\mu r^2 \dot{\psi} = \mu b \upsilon_\ell. \tag{1.66}$$

Substituting from Eq. (1.66) into Eq. (1.63) to eliminate $\dot{\psi}$ and solving for $\dot{r}$, we obtain:

$$\dot{r} = \left(\frac{2}{\mu}\right)^{1/2} \left[\eta E_\mathrm{i}\left(1 - \frac{b^2}{r^2}\right) - V(r)\right]^{1/2}. \tag{1.67}$$

The algebra for this step is as follows. Multiplying out the terms of Eq. (1.63) gives:

$$\eta E_\mathrm{i} - \frac{1}{2}\mu \dot{r}^2 = \frac{1}{2}\mu \frac{\upsilon_\ell^2 b^2}{r^2} + V(r),$$

and rearranging gives:

$$\eta E_\mathrm{i} - \frac{1}{2}\mu \frac{\upsilon_\ell^2 b^2}{r^2} = \frac{1}{2}\mu \dot{r}^2 + V(r). \tag{1.68}$$

Recall that $E_\mathrm{i} = 1/2 M_1 \upsilon_\ell^2$ and therefore $\upsilon_\ell^2 = 2E_\mathrm{i}/M_1$, and we can eliminate υ_ℓ so that the second term on the left-hand side of Eq. (1.68) becomes $-\dfrac{\mu b^2 E_\mathrm{i}}{M_1 r^2}$. Since $\mu = \dfrac{M_1 M_2}{M_1 + M_2}$ and $\mu/M_1 = \eta$, then:

$$\eta E_\mathrm{i} - \eta E_\mathrm{i} \frac{b^2}{r^2} = \frac{\mu \dot{r}^2}{2} + V(r), \quad \text{and} \quad \eta E_\mathrm{i}\left(1 - \frac{b^2}{r^2}\right) = \frac{\mu \dot{r}^2}{2} + V(r),$$

or

$$\dot{r} = \left(\frac{2}{\mu}\right)^{1/2} \left[\eta E_\mathrm{i}\left(1 - \frac{b^2}{r^2}\right) - V(r)\right]^{1/2},$$

which is the same as in Eq. (1.67). Note that r reaches the distance of closest approach, ρ, when $\dot{r} = 0$. At this point:

$$V(\rho) = \eta E_\mathrm{i}\left(1 - \frac{b^2}{\rho^2}\right), \tag{1.69}$$

and $V_\mathrm{max} = \eta E_\mathrm{i}$ (at $b = 0$) which represents a "head-on" collision. So if a particle strikes a target atom of equal mass, then $V_\mathrm{max} = 1/2 E_\mathrm{i}$. When $r \to \infty$, $V(r) \to 0$ and $\dot{r}^2 = \left(\dfrac{2}{\mu}\right)\eta E_\mathrm{i}$, or $\dot{r}^2 = 2E_\mathrm{i}/M_1$, $E_\mathrm{i} = 1/2 M_1 \dot{r}^2$ (and $\dot{r} = \upsilon_\ell$ at $r \to \infty$), so $E_\mathrm{i} = 1/2 M_1 \upsilon_\ell^2$.

Recall that we are looking for ϕ as a function of b. Going back to Eq. (1.67) and dividing $\dot{r}$ in Eq. (1.67) by $\dot{\psi}$ from Eq. (1.66), we have:

$$\frac{\dot{r}}{\dot{\psi}} = \frac{\mathrm{d}r}{\mathrm{d}\psi} = -\left(\frac{2}{\mu}\right)^{1/2}\left[\mu E_\mathrm{i}\left(1 - \frac{b^2}{r^2}\right) - V(r)\right]^{1/2}\frac{r^2}{\upsilon_\ell b}. \tag{1.70}$$

The minus sign in front of the quantity to the right of the equality is because for the first half of the orbit, $\dot{r}$ decreases as ψ increases. Bringing the term r^2 under the square root gives:

$$\frac{\mathrm{d}r}{\mathrm{d}\psi} = -\frac{1}{\upsilon_\ell b}\left(\frac{2}{\mu}\right)^{1/2}\left[\mu E_\mathrm{i}(r^4 - r^2b^2) - r^4V(r)\right]^{1/2}. \tag{1.71}$$

Dividing the terms under the square root by $\eta E_\mathrm{i}b^2$ to bring this term out of the square root gives:

$$\frac{\mathrm{d}r}{\mathrm{d}\psi} = -\frac{1}{\upsilon_\ell b}\left(\frac{2}{\mu}\right)^{1/2}(\eta E_\mathrm{i})^{1/2}b\left[\frac{r^4}{b^2}\left(1 - \frac{V(r)}{\eta E_\mathrm{i}}\right) - r^2\right]^{1/2}. \tag{1.72}$$

Since $1/2M_1\upsilon_\ell^2 = E_\mathrm{i}$, then $\upsilon_\ell = (2E_\mathrm{i}/M_1)^{1/2}$, and substituting for υ_ℓ gives:

$$\begin{aligned}\frac{\mathrm{d}r}{\mathrm{d}\psi} &= -\left(\frac{2}{\mu}\frac{M_1}{2E_\mathrm{i}}\eta E_\mathrm{i}\right)^{1/2}\left[\frac{r^4}{b^2}\left(1 - \frac{V(r)}{\eta E_\mathrm{i}}\right) - r^2\right]^{1/2} \\ &= -\left(\frac{M_1}{\mu}\eta\right)^{1/2}\left[\frac{r^4}{b^2}\left(1 - \frac{V(r)}{\eta E_\mathrm{i}}\right) - r^2\right]^{1/2} \\ &= -\left[\frac{r^4}{b^2}\left(1 - \frac{V(r)}{\eta E_\mathrm{i}}\right) - r^2\right]^{1/2}.\end{aligned} \tag{1.73}$$

Substituting for $x = 1/r$ gives:

$$\frac{\mathrm{d}x}{\mathrm{d}\psi} = \left[\frac{1}{b^2}\left(1 - \frac{V(x)}{\eta E_\mathrm{i}}\right) - x^2\right]^{1/2}. \tag{1.74}$$

This is the equation of orbit [$\psi = f(x)$].

The scattering angle ϕ is found by expressing $\mathrm{d}\psi$ as a function of x and $\mathrm{d}x$ and integrating from the limits on ψ corresponding to $x = 0$ and $1/\rho$. These limits are $\phi/2$

and $\pi/2$, respectively, as shown in Fig. 1.10. Performing this integration for the first half of the orbit yields:

$$\int_{\phi/2}^{\pi/2} \mathrm{d}\psi = \int_{0}^{1/\rho} \left[\frac{1}{b^2}\left(1 - \frac{V(x)}{\eta E_\mathrm{i}}\right) - x^2\right]^{-1/2} \mathrm{d}x, \tag{1.75}$$

and

$$\phi = \pi - 2\int_{0}^{1/\rho} \left[\frac{1}{b^2}\left(1 - \frac{V(x)}{\eta E_\mathrm{i}}\right) - x^2\right]^{-1/2} \mathrm{d}x. \tag{1.76}$$

The quantity ρ in the upper limit of x is the value of r when $\psi = \pi/2$ and hence is the distance of closest approach. Since $\mathrm{d}x/\mathrm{d}\psi = 0$ when $\psi = \pi/2$, ρ is given from Eq. (1.74) by:

$$\eta E_\mathrm{i} = \frac{V(\rho)}{1 - \dfrac{b^2}{\rho^2}}. \tag{1.77}$$

Equations (1.76) and (1.77) provide the relation between ϕ and b.

We have yet to determine the cross section for our scattering event. This may be done as follows. If particles M_1 are bombarding target atoms M_2, then in Fig. 1.11, those ions which cross an area $2\pi b\mathrm{d}b$ enclosed by circles of radii b and $b + \mathrm{d}b$ will be scattered into $\mathrm{d}\phi$ about ϕ. Since the relation between $\mathrm{d}b$ and $\mathrm{d}\phi$ can be obtained from Eq. (1.76) by differentiation, the differential cross section is given by:

$$\sigma_\mathrm{s}(E_\mathrm{i}, T)\mathrm{d}T = 2\pi b\mathrm{d}b \quad \text{and} \quad \sigma_\mathrm{s}(E_\mathrm{i}, T) = 2\pi b\frac{\mathrm{d}b}{\mathrm{d}\phi}\frac{\mathrm{d}\phi}{\mathrm{d}T}. \tag{1.78}$$

Knowing $V(r)$ enables ϕ to be written in terms of b^2 using Eq. (1.76) and then in terms of T using Eq. (1.13). Differentiating gives $2\pi b\mathrm{d}b$ as a function of T and $\mathrm{d}T$.

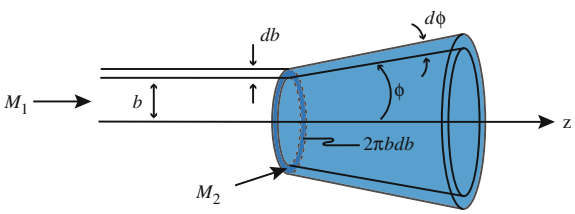

Fig. 1.11 Scattering of ions crossing an area $2\pi b\mathrm{d}b$ into an angular element $\mathrm{d}\phi$ about ϕ

Then from Eq. (1.78), the differential cross section for collisions having recoils in dT about T follows. The total cross section for collisions with T anywhere in the range $\check{T}$ to γE_i is as follows:

$$\sigma(E_i) = \int_{\check{T}}^{\gamma E_i} \sigma_s(E_i, T)\mathrm{d}T. \tag{1.79}$$

The process for finding the energy transfer cross section can be summarized as follows:

1. Select a potential function $V(r)$.
2. Use Eq. (1.76) to obtain b as a function of ϕ, $b = f(\phi)$.
3. Use Eq. (1.13) to obtain ϕ as a function of T, $\phi = g(T)$.
4. Use the relations between b and ϕ and between ϕ and T in Eq. (1.78) to obtain the energy transfer cross section.

The preceding description of the energy transfer cross section emphasizes the importance of knowing the potential function describing the particular ion–atom or atom–atom interaction of interest. Without accurate knowledge of the potential function, further description of the collision process and the ensuing defect structure become impossible. Unfortunately, explicit evaluation of the integral in Eq. (1.76) is possible only for simple potential functions. But before looking further at the various potential functions and their application in determining the energy transfer cross section, we must first consider the different possible classes of ions and their corresponding energies.

Classification of Ions

There are three important classes of ions in ion–atom collisions. The first is light energetic ions with $E_i > 1$ MeV. The second is highly energetic ($E_i \sim 10^2$ MeV) heavy ions such as fission fragments ($M \sim 10^2$). The third is lower energy heavy ions that may be produced by an accelerator or appear as a recoil that results from an earlier high-energy collision. The energy of these recoils is generally less than 1 MeV.

For each of these interactions, we must decide on the most appropriate potential function. A convenient guide is ρ/a, the ratio of the distance of closest approach to the screening radius as a function of the recoil energy, T. A rough graph of ρ/a versus T is provided in Fig. 1.12 to aid in the selection of the most appropriate potential. The three curves represent ions of each of the three classes just discussed: (1) 20 MeV protons, (2) 70 MeV fission fragments, and (3) 50 keV Cu ions. Curve (1) collisions apply to the regime where $\rho \ll a$ and the simple Coulomb potential is adequate. Curve (2) collisions that are head-on will have $\rho \ll a$ also. But for glancing collisions, $\rho \sim a$ and the screened Coulomb potential is most appropriate. Curve (3) represents the

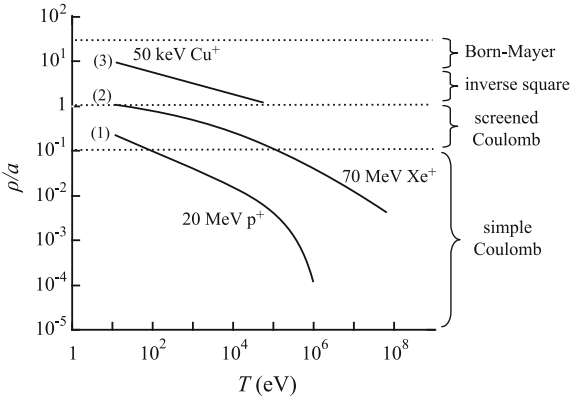

Fig. 1.12 Distance of closest approach ρ/a, as a function of T for (*1*) 20 MeV protons in Cu, (*2*) 70 MeV Xe^+ ions in Cu, and (*3*) 50 keV Cu^+ recoils in Cu (from [12])

region where $a < \rho \ll 5a$ and the inverse square potential or Brinkman potential would apply since both the Born–Mayer and screened Coulomb terms must be accounted for.

Hard Sphere-Type Collisions

The hard sphere potential is appropriate for ion energies below about 50 keV and for near head-on elastic collisions. Here, $\rho \sim r_e$ and atoms will act like hard spheres. In a head-on collision, $b = 0$ and from Eq. (1.77), we have:

$$\eta E_i = V(\rho). \tag{1.80}$$

When b is not quite zero, the collision may be pictured as shown in Fig. 1.13 where we define $R_1 = \rho \dfrac{M_2}{M_1 + M_2}$ and $R_2 = \rho \dfrac{M_1}{M_1 + M_2}$. If ρ is known, then from the figure:

$$b = \rho \cos \frac{\phi}{2}. \tag{1.81}$$

Now, recalling that:

$$\begin{aligned} \sigma_s(E_i, T)\, dT &= 2\pi b\, db \\ \sigma_s(E_i, T) &= 2\pi b \frac{db}{d\phi}\frac{d\phi}{dT}, \end{aligned} \tag{1.82}$$

where $\dfrac{db}{d\phi} = 1/2\rho \sin \phi/2$ from $b = \rho \cos \phi/2$ (using the absolute value of the derivative to maintain $\dfrac{db}{d\phi}$ as a positive value) and $\dfrac{d\phi}{dT} = \dfrac{2}{\gamma E_i \sin \phi}$ from $T = \dfrac{\gamma E_i}{2}(1 - \cos \phi)$. Then $\sigma_s(E_i, T) = 2\pi\rho \cos \phi/2 \dfrac{\rho}{2} \sin \phi/2 \dfrac{2}{\gamma E_i \sin \phi}$, and

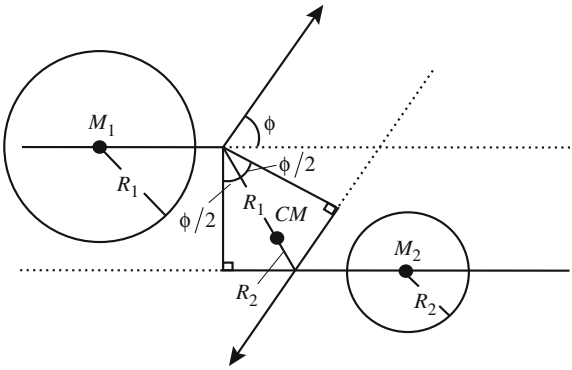

Fig. 1.13 Schematic of colliding atoms obeying the hard sphere approximation for collisions

$$\sigma_s(E_i, T) = \frac{\pi\rho^2}{\gamma E_i}. \tag{1.83}$$

Recall that for neutron–nuclear interactions, $\sigma_s(E_i, T) = \sigma_s(E_i)/\gamma E_i$. Using this relation, we can obtain an idea of the size of the energy transfer cross section for neutron–nuclear interactions versus atom–atom interactions: $\frac{\sigma_s(E_i,T)^{a-a}}{\sigma_s(E_i,T)^{\text{n-nuclear}}} = \frac{\pi\rho^2}{\sigma_s(E_i)} \sim \frac{\pi(10^{-8})^2}{10^{-24}} \sim 10^8$, and so the energy transfer cross section for atom–atom interactions is about eight orders of magnitude greater than that for neutron–nuclear interactions.

The total scattering cross section is as follows:

$$\sigma_s(E_i) = \int_{\check{T}}^{\gamma E_i} \sigma_s(E_i, T)\mathrm{d}T = \int_{\check{T}}^{\gamma E_i} \frac{\pi\rho^2}{\gamma E_i}\mathrm{d}T = \frac{\pi\rho^2}{\gamma E_i}[\gamma E_i - \check{T}] = \pi\rho^2. \tag{1.84}$$

Note that $\sigma_s(E_i)$ is independent of E_i (because $\rho \neq f(E_i)$) and that $\sigma_s(E_i, T) \propto 1/E_i$ and is independent of T. We can find $\sigma_s(E_i, T)$ explicitly by applying the appropriate potential function to find a value of ρ (determined by $V(r)$). Recall from our discussions in Sect. 1.2.1 that for collisions in which the impact parameter is on the order of the equilibrium separation of the atoms, the Born–Mayer potential is most appropriate. This corresponds to energies below about 10 keV. (Note that this means that we are also backing off from a pure hard sphere model.) Hence, we will use $V(r) = A\exp(-r/B)$, where A and B are defined in Eq. (1.47). Using Eq. (1.80) gives:

$$V(\rho) = A\exp(-\rho/B) = \eta E_i, \tag{1.85}$$

or

$$\rho = B \ln\left(\frac{A}{\eta E_\mathrm{i}}\right), \tag{1.86}$$

and since $b = \rho \cos \phi/2 = B\ln(A/\eta E_\mathrm{i})\cos \phi/2$, the energy transfer cross section is as follows:

$$\sigma_\mathrm{s}(E_\mathrm{i}, T) = \frac{\pi B^2}{\gamma E_\mathrm{i}} \left[\ln \frac{A}{\eta E_\mathrm{i}}\right]^2. \tag{1.87}$$

The total scattering cross section is then the integral of the energy transfer cross section between the limits $\check{T}$ and γE_i:

$$\sigma_\mathrm{s}(E_\mathrm{i}) = \int_{\check{T}}^{\gamma E_\mathrm{i}} \pi B^2 \left[\ln \frac{A}{\eta E_\mathrm{i}}\right]^2 \frac{1}{\gamma E_\mathrm{i}} \mathrm{d}T. \tag{1.88}$$

From this expression, we will be able to calculate the total cross section for displacement scattering events for all allowed T. Note that the total scattering cross section depends on E_i. Also, for typical values of A, B, and $\check{T}$ (40 eV), the value of $\sigma_\mathrm{s}(E_\mathrm{i})$ for atom–atom interactions is about 10^8 times that for neutron–nuclear events.

Rutherford Scattering

Let us turn now to a second example in which we will use the pure Coulomb scattering potential to demonstrate Rutherford scattering. From our classification of ions according to ion energy and mass, type 1 collisions involve light ($m \sim$ 1–4) energetic ($E >$ MeV) ions where $\rho \ll a$. Collisions of this sort are adequately represented by the simple Coulomb potential, which from Eq. (1.48) is as follows:

$$V(r) = \frac{Z_1 Z_2 \varepsilon^2}{r}.$$

We will assume that Z_1 and Z_2 represent the nuclear charges and that this collision occurs at high energies so that electrons are stripped from the nuclei and the only interaction is between the nuclei.

In our description of the trajectories of the particles in the CM system, we found that at the point of closest approach, $\mathrm{d}x/\mathrm{d}\psi = 0$ and from Eq. (1.77):

$$\eta E_\mathrm{i} = \frac{V(\rho)}{1 - \dfrac{b^2}{\rho^2}}.$$

Substituting in for $V(r)$ gives:

$$\frac{Z_1 Z_2 \varepsilon^2}{\rho} = \eta E_\mathrm{i}\left(1 - \frac{b^2}{\rho^2}\right). \tag{1.89}$$

Defining:

$$b_0 = \left(\frac{Z_1 Z_2 \varepsilon^2}{\eta E_\mathrm{i}}\right), \tag{1.90}$$

it follows that:

$$\frac{b_0}{\rho} = 1 - \frac{b^2}{\rho^2}, \tag{1.91}$$

and

$$\rho = \frac{b_0}{2}\left[1 + \left(1 + \frac{4b^2}{b_0^2}\right)^{1/2}\right]. \tag{1.92}$$

Hence, the distance of closest approach is a function of the impact parameter b, as expected. For head-on collisions, $b = 0$ and the minimum value of ρ depends on E_i:

$$\rho(b = 0) = \rho_0 = b_0 = \frac{Z_1 Z_2 \varepsilon^2}{\eta E_\mathrm{i}}. \tag{1.93}$$

Note that for this type of collision, ρ depends on E_i, in contrast to independence of E_i in the hard sphere model. Going back to the orbital Eq. (1.75), we will now evaluate it as a definite integral:

$$\int_{\pi/2}^{\phi/2} \mathrm{d}\psi = \int_{1/\rho}^{0} \left[\frac{1}{b^2} - \frac{b_0}{b^2}x - x^2\right]^{-1/2} \mathrm{d}x. \tag{1.94}$$

Since $\psi = \pi/2$ when $r = \rho(x = 1/\rho)$ and $\psi = \phi/2$ when $r = \infty$ $(x = 0)$, letting $y = x + \dfrac{b_0}{2b^2}$ gives:

$$\phi/2 - \pi/2 = \int_{\frac{1}{\rho} + \frac{b_0}{2b^2}}^{\frac{b_0}{2b^2}} [c^2 - y^2]^{-1/2} \mathrm{d}y, \tag{1.95}$$

where $c^2 = \left(\frac{1}{b^2} + \frac{b_0^2}{4b^4}\right)$. The orbits are then as follows:

$$\begin{aligned}\phi/2 - \pi/2 &= \left[\sin^{-1}\frac{y}{c}\right]_{\frac{1}{\rho}+\frac{b_0}{2b^2}}^{\frac{b_0}{2b^2}} \\ &= \sin^{-1}\frac{b_0}{2b^2 c} - \sin^{-1}\frac{1}{c}\left(\frac{1}{\rho} + \frac{b_0}{2b^2}\right).\end{aligned} \tag{1.96}$$

Since $\sin^{-1}\frac{1}{c}\left(\frac{1}{\rho} + \frac{b_0}{2b^2}\right) = \sin^{-1}(1) = \pi/2$, then:

$$\sin\phi/2 = \frac{b_0}{2b^2 c}. \tag{1.97}$$

Substituting for c (from above) into Eq. (1.97) yields:

$$\sin^2\phi/2 = \frac{1}{1 + \frac{4b^2}{b_0^2}}. \tag{1.98}$$

Using trigonometric relations for $\sin^2\phi/2$, we have:

$$b = \frac{b_0}{2}\cot\phi/2. \tag{1.99}$$

We now have a relationship between the impact parameter, b, and the asymptotic scattering angle, ϕ. Note that b is a function of E_i through b_0 (Eq. (1.93)).

We now want an expression for the scattering cross section. Using Eq. (1.82) for $\sigma_\mathrm{s}(E_\mathrm{i}, T)$, we have:

$$\sigma_\mathrm{s}(E_\mathrm{i}, T)\,\mathrm{d}T = \sigma_\mathrm{s}(E_\mathrm{i}, \phi)\,\mathrm{d}\Omega = 2\pi b\mathrm{d}b = \pi b_0 \cot\frac{\phi}{2}\,\mathrm{d}b, \tag{1.100}$$

and substituting for db from Eq. (1.99) gives:

$$\sigma_\mathrm{s}(E_\mathrm{i}, \phi) = \left(\frac{b_0}{4}\right)^2 \frac{1}{\sin^4(\phi/2)}, \tag{1.101}$$

which is the Rutherford inverse fourth power scattering law. The cross section for recoil is exactly the same as for elastic collisions, Eq. (1.13), and since:

$$\sigma_\mathrm{s}(E_\mathrm{i}, T) = \sigma_\mathrm{s}(E_\mathrm{i}, \phi)\frac{\mathrm{d}\Omega}{\mathrm{d}T},$$

we have:

$$\sigma_s(E_i, T) = \frac{\pi b_0^2}{4} \frac{\gamma E_i}{T^2}. \tag{1.102}$$

Note that unlike neutron–nuclear collisions and hard sphere scattering in general, the Rutherford scattering cross section is a strong function of T. This expression also shows that the scattering cross section $\sigma_s(E_i, T) \rightarrow \infty$ as $T \rightarrow 0$. But this is just a reflection of the fact that as $\phi \rightarrow 0$ and $b \rightarrow \infty$ and is representative of long-range Coulomb interactions. In reality, there is a cutoff in b and hence in ϕ due to electron screening. As we will see later, this cutoff is E_d, the displacement energy. The average energy transferred is then as follows:

$$\overline{T} = \frac{\int_{\check{T}}^{\hat{T}} T\sigma_s(E_i, T)\,dT}{\int_{\check{T}}^{\hat{T}} \sigma_s(E_i, T)\,dT} = \frac{\check{T}\ln(\hat{T}/\check{T})}{1 - \frac{\check{T}}{\hat{T}}}. \tag{1.103}$$

For $\hat{T} = \gamma E_i$ and $\check{T} = E_d$ and since $\gamma E_i \gg E_d$, then:

$$\overline{T} \approx E_d \ln\left(\frac{\gamma E_i}{E_d}\right), \tag{1.104}$$

which is quite small for all energies E_i, reflecting the strong T^{-2} dependence in Eq. (1.102).

The integral of Eq. (1.102) over T gives the total cross section for displacement events by an ion of energy E_i:

$$\sigma_s(E_i) = \frac{\pi}{4} b_0^2 \hat{T} \int_{E_d}^{\hat{T}} \frac{dT}{T^2} = \frac{\pi b_0^2}{4}\left(\frac{\hat{T}}{E_d} - 1\right), \tag{1.105}$$

and since at high energies $\hat{T}/E_d \gg 1$ then we have for $\hat{T} = \gamma E_i$:

$$\sigma_s(E_i) \approx \frac{\pi b_0^2}{4} \frac{\gamma E_i}{E_d}, \tag{1.106}$$

which is quite large.

A critical question in applying the above results is under what conditions can Rutherford scattering be applied? The answer is that we must require that during an

encounter, the major part of scattering occurs in the region where $r \ll a$ But this is a qualitative measure. What is needed is a means for determining quantitatively, when Rutherford scattering applies. To address this question, we consider two cases.

Case 1: Near "head-on" collisions (*high T*). For near head-on collision, $\rho_0 \ll a$ or $E_\mathrm{i} \gg E_a$, where E_a is the value of E_i that would give $\rho_0 = a$ assuming a screened Coulomb potential:

$$E_a = \frac{2E_\mathrm{R}}{C}(Z_1 Z_2)^{7/6}\frac{M_1 + M_2}{M_2 e}, \tag{1.107}$$

which is obtained by rewriting the screened Coulomb potential (Eq. (1.49)) in an inverse square law form (Eq. (1.59)), with $\varepsilon^2 = 2a_0 E_\mathrm{R}$ and equating at $r = a$ and setting $V(r) = \eta E_\mathrm{i} = \dfrac{M_2}{M_1 + M_2}E_\mathrm{i}$ for a head-on collision.

Case 2: Glancing collisions (*low T*). Here, we only consider those collisions in which $b \le a$, or that result in an energy transfer $\check{T} \sim E_\mathrm{d}$ for $b = a$. For a simple Coulomb collision with $b = a$, we have from Eqs. (1.98) and (1.13):

$$T = \frac{e^2\gamma E_a^2}{4E_\mathrm{i}}, \text{ or } E_\mathrm{i} = \frac{e^2\gamma E_a^2}{4T}, \tag{1.108}$$

and giving this value of E_i the name E_b at $T = \check{T}$, we have

$$E_b = \frac{e^2\gamma E_a^2}{4\check{T}}, \quad \text{where} \quad \check{T} = E_\mathrm{d}, \tag{1.109}$$

and this equation is valid for all $E_\mathrm{i} \gg E_b$. Essentially, E_b is the value of E_i that results in a transfer of energy $T \ge E_\mathrm{d}$ at $b = a$. Or looking at it another way, values of $E_b < E_\mathrm{i}$ give $T \ll \check{T}$ and can be neglected since $\rho \ge a$, and these encounters can be neglected. Table 1.4 provides examples of the values of E_a and E_b for different particle–target atom combinations and energies. From Table 1.4, since $E_a < E_b$, we can use the criterion that E_i must be $\gg E_b$ as an extreme test of the validity of the simple Coulomb scattering description.

In summary, if $E_\mathrm{i} \gg E_a$, the simple Coulomb potential may be used for near head-on collisions. If $E_\mathrm{i} \gg E_b$, it can be used for all collisions of interest in radiation damage. Light charged particles such as protons and alphas with $E_\mathrm{i} > 1$ MeV fall into this category, while fission fragments are in the regime $E_a < E_\mathrm{i} < E_b$ and recoils have $E_\mathrm{i} \le \mathrm{E}_a$. These will be discussed next. But first, we present an example of Rutherford scattering.

Table 1.4 Values of E_a and E_b for various particle–target atom combinations and energies (from [13])

Incident particle	Target atom	E_a (eV)	E_b (eV)
C	C	2×10^3	8×10^5
Al	Al	1×10^4	2×10^7
Cu	Cu	7×10^4	1×10^9
Au	Au	7×10^5	1×10^{11}
Xe	U	5×10^5	3×10^{10}
D	C	1.5×10^2	2×10^3
D	Cu	1×10^3	2×10^4
D	C	4×10^3	1×10^5

Example 1.2. 2 MeV protons on aluminum
For this case,

$$\hat{T} = \gamma E_\mathrm{i} = \frac{4(27)}{(27+1)^2} 2\,\mathrm{MeV} = 0.28\,\mathrm{MeV}$$

$$\check{T} = 40\,\mathrm{eV}$$

$$\overline{T} = E_\mathrm{d} \ln\left(\frac{\gamma E_\mathrm{i}}{E_\mathrm{d}}\right) = 354\,\mathrm{eV}$$

We can also calculate $E_a \sim 200$ eV and $E_b \sim 2500$ eV. (For comparison, 2 MeV He^+ on Al, $E_a \sim 1$ keV, and $E_b \sim 16$ keV. Also, for 2 MeV H^+ on Au, $E_a \sim 1.6$ keV, and $E_b \sim 24$ keV; and for 2 MeV He^+ on Au, $E_a \sim 8$ keV, and $E_b \sim 42$ keV.) Since $E_\mathrm{i} \gg E_b$, the simple Coulomb law is valid for this type of collision. Incidentally, $\sigma(E_\mathrm{i}) \sim 4 \times 10^{-22}$ cm^2, and since the mean free path between collisions is $\lambda = 1/\sigma N$ and $N \sim 6 \times 10^{22}$ a/cm^3, then $\lambda \sim 0.04$ cm or about 400 μm, or about 10 times the length of a 2 MeV proton track in Al. This means that there is, on average, only one Rutherford scattering collision for every 10 protons incident on Al.

Now, let us investigate the other classes of ion–atom collisions such as heavy energetic ions, heavy slow ions, and high-energy electrons.

Heavy Energetic Ions

For heavy energetic ions such as fission fragments, Fig. 1.12 shows that an appropriate potential must account for both screened Coulomb and closed shell repulsion. Let us look first at the simple Coulomb potential as a rough approximation, knowing that its use is only justified for recoil energies approaching γE_i where $\rho \ll a$. Recall that $\sigma_\mathrm{s}(E_\mathrm{i}) = \frac{\pi b_0^2}{4}\frac{\gamma E_\mathrm{i}}{E_\mathrm{d}}$, and $b_0 \propto \frac{Z_1}{\gamma E_\mathrm{i}}, \gamma = \frac{4M_1M_2}{(M_1+M_2)^2}, \eta = \frac{M_2}{M_1+M_2}$, which gives an increase in the cross section compared to the light ion by a factor of

$$\frac{\sigma_{\mathrm{s,heavy}}}{\sigma_{\mathrm{s,light}}} = \frac{\left.\frac{z_1^2 M_1}{E_\mathrm{i}}\right|_{\mathrm{heavy}}}{\left.\frac{z_1^2 M_1}{E_\mathrm{i}}\right|_{\mathrm{light}}} \approx 10^6$$

for the same value of E_i and for fission fragments at the peaks of the fission yield of uranium, $M_1^{\mathrm{light}} \simeq 96$ amu, $E_1^{\mathrm{light}} \simeq 95$ MeV and $M_1^{\mathrm{heavy}} \simeq 137$ amu, $E_1^{\mathrm{heavy}} \simeq 55$ MeV. Comparing to the example of the 2 MeV proton on Al, fission fragments have a cross section that is larger by a factor of 10^4! Therefore, the mean free path is 10^{-4} that of a proton in Al.

Recall that $\sigma_\mathrm{s}(E_\mathrm{i}, T)$ varies as $1/T^2$. But this is only true near $\gamma E_\mathrm{i}(\rho \ll a)$. At lower energies, screening will reduce the sensitivity to energy. So we must use a better description of the interaction between energetic, heavy ions, and target atoms. Brinkman's expression, Eq. (1.50), includes both terms, and if this is used in the impulse approximation (see [13]), the result is as follows:

$$T = \frac{M_1}{M_2}\frac{A^2}{E_\mathrm{i}}\left[F\left(\alpha, \frac{b}{B}\right) - (1-\alpha)F\left(1+\alpha, \frac{b}{B}\right)\right]^2, \tag{1.110}$$

where A and B are given in Eq. (1.50) and

$$\begin{aligned} F\left(\alpha, \frac{b}{B}\right) &= \frac{b}{B}\int_{b/a}^{\infty} \frac{-e^{-x}\mathrm{d}x}{\left(x^2 - b^2/a^2\right)^{1/2}\left(1-e^{-\alpha x}\right)^2} \\ &= \frac{b}{B}\sum_{n=0}^{\infty}(n+1)K_0\left\{\frac{b}{B}(1+n\alpha)\right\}, \end{aligned} \tag{1.111}$$

where $K_0(y)$ is a Bessel function of the third kind. The term α is the ratio of Born–Mayer and screened Coulomb terms at $r = a$, so in general, $\alpha < 1$. T can be found from b and Eq. (1.110), and by inversion, b is obtained as a function of T. Differentiation gives $\sigma = 2\pi b\mathrm{d}b$. However, because of the complexity of Eq. (1.110), numerical solutions are required. Nevertheless, we may calculate dN, the number of recoils in dT at T produced by the fission fragment in slowing down to rest. This is found by:

$$\mathrm{d}N = n\sigma\mathrm{d}x = n\frac{\mathrm{d}\sigma}{\mathrm{d}T}\left(-\frac{\mathrm{d}E}{\mathrm{d}x}\right)^{-1}\mathrm{d}E\mathrm{d}T, \tag{1.112}$$

where n is the density of atoms, and

$$N(T)\mathrm{d}T = n\int_0^{E_\mathrm{i}} \frac{\sigma}{\mathrm{d}T}\left(\frac{\mathrm{d}E}{\mathrm{d}X}\right)^{-1}\mathrm{d}E\,\mathrm{d}T. \tag{1.113}$$

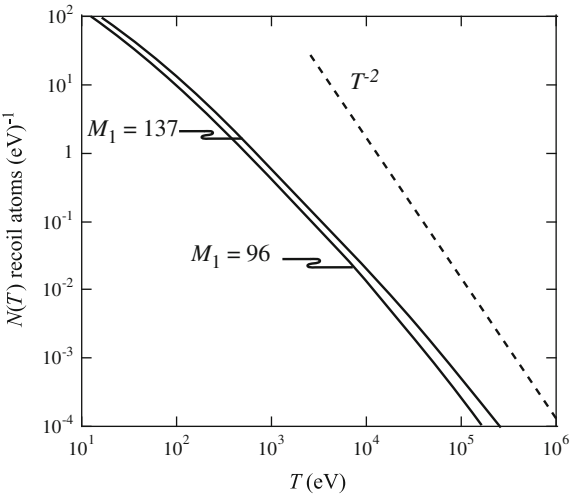

Fig. 1.14 The energy spectrum of recoils $N(T)$ dT produced by fission fragments slowing down to rest in uranium. Two cases are shown: $M_1 = 96$, $E_1 = 95$ MeV; and $M_1 = 137$, $E_1 = 55$ MeV (from [13])

Brinkman carried out these calculations for light and heavy fragments from ^{235}U fission slowing down in uranium. The results are shown in Fig. 1.14. Note that $N(T)$ decreases more rapidly than T^{-1}, and hence, the majority of displaced atoms are produced by low-energy recoils. Therefore, high-energy recoils can be neglected altogether. Another way of looking at this is that the simple Coulomb potential is only valid in an energy range that does not contribute significantly to displacements.

Heavy Slow Ions

These ions are classified by the curve labeled "3" as shown in Fig. 1.12. This is a very important class of collisions as it covers most of the applications of kV ion implanters and low MV accelerators in the fields of materials science and radiation damage that includes such topics as ion implantation and heavy ion radiation effects simulation. The figure shows that collisions must be dealt with over the range $a < \rho < 10a$. The formalism used for fission fragments in the previous section applies to glancing collisions, but for head-on collisions, another approach is needed. The appropriate potential for $a/5 \leq \rho \leq 5a$ is the inverse square approximation. We use a potential of the form:

$$V(r) = \frac{2E_R}{e}(Z_1 Z_2)^{5/6}\left(\frac{a_0}{r}\right)^2,$$

which is obtained by fitting a screened Coulomb potential to the inverse square potential and equating at $r = a$, Eq. (1.59). Substituting this potential function into the orbital equation (1.76) gives:

$$\frac{\phi}{\pi} = 1 - \left(1 + \frac{a^2 E_a}{b^2 E_\mathrm{i}}\right)^{-1/2}. \tag{1.114}$$

Using Eq. (1.13) to express ϕ in terms of T gives:

$$T = \gamma E_\mathrm{i} \cos^2\left[\frac{\pi}{2}\left(1 + \frac{a^2 E_a}{b^2 E_\mathrm{i}}\right)^{-1/2}\right]. \tag{1.115}$$

Expressing b in terms of T and differentiating gives:

$$\sigma_\mathrm{s}(E_\mathrm{i}, T) = \frac{4E_a a^2 \alpha}{\gamma E_\mathrm{i}^2 (1 - 4\alpha^2)^2 [x(1-x)]^{1/2}}, \tag{1.116}$$

where $x = \dfrac{T}{\gamma E_\mathrm{i}}$ and $\pi\alpha = \cos^{-1} x^{1/2}$.

For small x (low-energy transfer), we have:

$$\sigma_\mathrm{s}(E_\mathrm{i}, T) = \frac{\pi^2 a^2 E_a \gamma^{1/2}}{8 E_\mathrm{i}^{1/2} T^{3/2}}. \tag{1.117}$$

Note that the energy transfer cross section is dependent on T. The mean recoil energy is as follows:

$$\overline{T} = \frac{\int_{\check{T}}^{\gamma E_\mathrm{i}} T\sigma_\mathrm{s}(E_\mathrm{i}, T)\,\mathrm{d}T}{\int_{\check{T}}^{\gamma E_\mathrm{i}} \sigma_\mathrm{s}(E_\mathrm{i}, T)\,\mathrm{d}T} = (\gamma E_\mathrm{i} \check{T})^{1/2}. \tag{1.118}$$

The total cross section for displacement is as follows:

$$\sigma_\mathrm{s}(E_\mathrm{i}) = \int_{\check{T}}^{\gamma E_\mathrm{i}} \sigma_\mathrm{s}(E_\mathrm{i}, T)\,\mathrm{d}T = \frac{\pi^2 a^2 E_a \gamma^{1/2}}{4(E_\mathrm{i}\check{T})^{1/2}}. \tag{1.119}$$

Relativistic Electrons

Radiation damage from electrons is not so important in reactor core materials, but more so in the laboratory as they are commonly used in electron microscopes for radiation damage studies. Due to the low mass of the electron, very high energies must be attained in order to cause displacements of a lattice atom. These energies are high enough such that relativistic quantum mechanics must be used to describe the collision. Even so, the energy transferred is large enough to displace only the struck atom with no secondary displacements.

In relativistic form, the momentum of an electron with rest mass m_0 and kinetic energy E_i is as follows:

$$p_\mathrm{e}^2 = \frac{E_\mathrm{i}}{c^2}(E_\mathrm{i} + 2m_0c^2). \tag{1.120}$$

Since the struck atom (Z, M) recoils non-relativistically, the recoil expression is that given in Eq. (1.9):

$$V_\ell'^2 = V_\mathrm{CM}^2 + V_\mathrm{c}'^2 - 2V_\mathrm{CM}V_\mathrm{c}'\cos\phi = 2V_\mathrm{CM}^2(1-\cos\phi) = 4V_\mathrm{CM}^2\sin^2\frac{\phi}{2},$$

and conservation of momentum gives:

$$p_\mathrm{e} = (m_0 + M)V_\mathrm{CM} \cong MV_\mathrm{CM}.$$

Replacing the velocity terms with energies in the expression for $V_\ell'^2$ yields:

$$T = \frac{2E_\mathrm{i}}{Mc^2}(E_\mathrm{i} + 2m_0c^2)\sin^2\frac{\phi}{2}, \tag{1.121}$$

or

$$\hat{T} = \frac{2E_\mathrm{i}}{Mc^2}(E_\mathrm{i} + 2m_0c^2). \tag{1.122}$$

An approximate expression for the Dirac equation for light ions [13] yields the differential scattering cross section:

$$\begin{aligned}\sigma_\mathrm{s}(E_1,\phi) = {} & \frac{4\pi a_0^2 Z^2 E_\mathrm{R}^2}{m_0^2c^4}\frac{1-\beta^2}{\beta^4} \\ & \times [1-\beta^2\sin^2(\phi/2) + \pi\alpha\beta\sin(\phi/2)(1-\sin(\phi/2))] \\ & \times \cos(\phi/2)\csc^3(\phi/2),\end{aligned} \tag{1.123}$$

where $\beta = \upsilon/c$ and $\alpha = Z_2/137$. This expression approaches the Rutherford scattering law for small β. Using Eqs. (1.121) and (1.122), the differential scattering cross section is written in terms of T and $\hat{T}$:

$$\sigma_\mathrm{s}(E_\mathrm{i},T) = \frac{4\pi a_0^2 Z^2 E_\mathrm{R}^2}{m_0^2c^4}\frac{1-\beta^2}{\beta^4}\left[1-\beta^2\frac{T}{\hat{T}} + \pi\frac{\alpha}{\beta}\left\{\left(\frac{T}{\hat{T}}\right)^{1/2} - \frac{T}{\hat{T}}\right\}\right]\frac{\hat{T}}{T^2}. \tag{1.124}$$

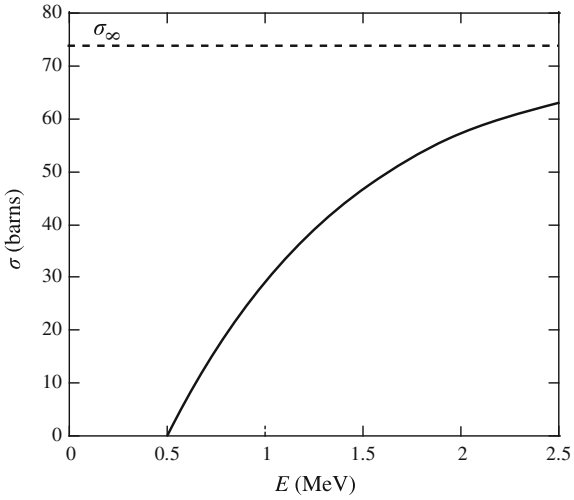

Fig. 1.15 Damage cross section for electrons bombarding copper where E_d = 25 eV (from [13])

The total cross section is found by integrating Eq. (1.124) from $\check{T}$ to $\hat{T}$:

$$\sigma_s(E_i) = \frac{4\pi a_0^2 Z^2 E_R^2}{m_0^2 c^4} \frac{1-\beta^2}{\beta^4} \left(\frac{\hat{T}}{\check{T}} - 1 \right) - \beta^2 \log \frac{\hat{T}}{\check{T}} + \alpha\beta 2 \left(\frac{\hat{T}}{\check{T}} \right)^{1/2} - 1 - \log \frac{\hat{T}}{\check{T}}. \tag{1.125}$$

For electrons with energies above the damage threshold and $\hat{T}/\check{T}$ slightly greater than unity:

$$\sigma_s(E_i) \cong \frac{4\pi a_0^2 Z^2 E_R^2}{m_0^2 c^4} \left(\frac{1-\beta^2}{\beta^4} \right)^2 \left(\frac{\hat{T}}{\check{T}} - 1 \right). \tag{1.126}$$

Figure 1.15 shows that at high enough energies, $E_i \gg m_0 c^2$, and $\sigma_s(E_i)$ approaches an asymptotic value:

$$\sigma_s(E_i) \to \frac{8\pi a_0^2 Z^2 E_R^2}{\check{T} M c^2} = \sigma_\infty. \tag{1.127}$$

It should be emphasized, however, that these cross sections are most accurate for light elements but seriously underestimate $\sigma_s(E_i)$ for heavy elements ($Z > 50$). Table 1.5 provides a summary of the energy transfer and the energy transfer cross sections for the various types of atom–atom interactions discussed in Sect. 1.2.

Table 1.5 Energy transfer and energy transfer cross sections for various types of atom–atom collisions

Type of collision	Energy transfer and energy transfer cross section	Equation in text
Hard sphere type (Born–Mayer potential) $\rho \sim r_e$	$\sigma_s(E_i, T) = \frac{\pi B^2}{\gamma E_i}\left[\ln\frac{A}{\eta E_i}\right]^2$	(1.87)
	$\overline{T} = \gamma E_i/2$	(1.13)
Rutherford scattering (simple Coulomb potential) $\rho \ll a$	$\sigma_s(E_i, T) = \frac{\pi b_0^2}{4}\frac{E_i\gamma}{T^2}$	(1.102)
	$\overline{T} \approx E_d \ln\left(\frac{\gamma E_i}{E_d}\right)$	(1.104)
Heavy ion (inverse square) $a/5 \le \rho \le 5a$	$\sigma_s(E_i, T) = \frac{\pi^2 a^2 E_a \gamma^{1/2}}{8E_i^{1/2}T^{3/2}}$	(1.117)
	$\overline{T} = \left(\gamma E_i \check{T}\right)^{1/2}$	(1.118)
Relativistic electrons	$\sigma_s(E_i, T) = \frac{4\pi a_0^2 Z^2 E_R^2}{m_0^2 c^4}\frac{1-\beta^2}{\beta^4} \times \left[1 - \beta^2\frac{T}{\hat{T}} + \pi\frac{\alpha}{\beta}\left\{\left(\frac{T}{\hat{T}}\right)^{1/2} - \frac{T}{\hat{T}}\right\}\right]\frac{\hat{T}}{T^2}$	(1.124)

1.3 Energy Loss

Up to this point, we have been treating collisions as discrete events. However, besides collision with or between nuclei, an ion or atom traveling through the lattice may lose energy by electronic excitation, by ionization, or by Bremsstrahlung (loss of energy of an electron passing through the Coulomb field of a nucleus by emission of X-rays). These events may be viewed as more or less continuous events. What follows is a treatment of energy loss in solids.

1.3.1 Energy Loss Theory

We are interested in finding the differential energy loss of an ion or atom traveling through a lattice. We begin by defining the energy loss per unit length as $-\mathrm{d}E/\mathrm{d}x$ (or $NS(E)$ where N is the target atom number density and S is the stopping power in units of energy × distance squared) so that the total energy loss can then be approximated by a sum of these components:

$$\left(-\frac{\mathrm{d}E}{\mathrm{d}x}\right)_{\text{total}} = \left(-\frac{\mathrm{d}E}{\mathrm{d}x}\right)_n + \left(-\frac{\mathrm{d}E}{\mathrm{d}x}\right)_e + \left(-\frac{\mathrm{d}E}{\mathrm{d}x}\right)_r = NS_n + NS_e + NS_r, \quad (1.128)$$

where the subscripts are defined as follows:
n = elastic,
e = electronic, and
r = radiation.

For most of the applications in which we will be interested, energy loss by radiation will be small and will be neglected.

From our discussion in Sect. 1.2.1, it is evident that in order to accurately describe the slowing down of an ion or atom over the entire energy range from $\hat{T}$ to $\check{T}$, where $\hat{T}$ may be in MeV and $\check{T} \sim 10$ eV, several potential functions would need to be "pieced" together (see Fig. 1.9). This would cause problems because of discontinuities at the cuts. Moreover, the cutoff points of these functions often differ depending on M and Z.

However, we can separate or subdivide stopping power according to the type of interaction and hence the energy regime. In the high-energy regime, $\rho \ll a$ and $S_e \gg S_n$, and these interactions are treated as pure Coulomb collisions. In the low-energy regime, $\rho \approx a$ and $S_n > S_e$. This is the region of importance in the deposition of displacement energy. In either case, we can establish a formalism for calculating stopping power, $-\mathrm{d}E/\mathrm{d}x = NS(E)$.

If we know the energy transfer cross section $\sigma(E_i, T)$ for either S_n or S_e, then we can calculate the average energy transfer:

$$\overline{T} = \frac{\int T\sigma \mathrm{d}T}{\int \sigma \mathrm{d}T} = \text{energy lost or transferred,}$$

and the mean free path (mfp) between collisions is $\lambda = \dfrac{1}{N\sigma}$. Then, the ratio of these two quantities is the energy loss per unit length:

$$\begin{aligned} \frac{\mathrm{d}E}{\mathrm{d}x} = NS_n = \frac{\overline{T}}{\lambda} &= \frac{\int_{\check{T}}^{\hat{T}} T\sigma(E_i, T)\,\mathrm{d}T}{\int_{\check{T}}^{\hat{T}} \sigma(E_i, T)\,\mathrm{d}T} \cdot N \int_{\check{T}}^{\hat{T}} \sigma(E_i, T)\,\mathrm{d}T \\ &= N \int_{\check{T}}^{\hat{T}} T\sigma(E_i, T)\,\mathrm{d}T. \end{aligned} \tag{1.129}$$

Another way to look at this is as follows: Consider a projectile incident on an amorphous target containing an average of N atoms/unit volume (Fig. 1.16). In traversing the slab of material between x and $x + \Delta x$, the projectile will come within a distance b_1 of $N\Delta x 2\pi b_1 \mathrm{d}b$ target particles and transfer an energy $T(E_i, b)$ to each.

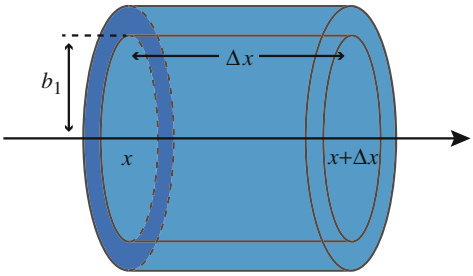

Fig. 1.16 Schematic of an incident projectile of energy E passing within a distance b_1 of an annular ring containing $N\Delta x 2\pi b_1 \mathrm{d}b$ atoms

The total energy transferred to all target particles in the slab is obtained by integrating over all possible impact parameters:

$$\Delta E = N\Delta x \int_0^\infty T 2\pi b \, \mathrm{d}b.$$

Assuming $\Delta E \ll E$ and dividing by Δx and taking the limit as $\Delta x \to 0$, we obtain:

$$\left.\frac{\Delta E}{\Delta x}\right|_{\lim \Delta x \to 0} = \frac{\mathrm{d}E}{\mathrm{d}x} = N \int_0^\infty T 2\pi b \, \mathrm{d}b.$$

We know that $\sigma\,(E_\mathrm{i},\, T)\,\mathrm{d}T = 2\pi b \mathrm{d}b$ so:

$$\frac{\mathrm{d}E}{\mathrm{d}x} = N \int_{\check{T}}^{\hat{T}} T\sigma(E_\mathrm{i}, T)\,\mathrm{d}T,$$

which is the same result as from Eq. (1.129). Let us first consider nuclear stopping, or energy loss from elastic collisions.

Nuclear Stopping Power

We define $\left(-\frac{\mathrm{d}E}{\mathrm{d}x}\right)_\mathrm{n}$ or $NS_\mathrm{n}(E_\mathrm{i})$ as the energy lost to target nuclei when a projectile of energy E_i traverses a differential thickness $\mathrm{d}x$ of a target of unit density. A simple formulation of $\left(-\frac{\mathrm{d}E}{\mathrm{d}x}\right)_\mathrm{n}$ can be made if we assume that each target nucleus acts independently of every other target nucleus in slowing down a projectile. In essence, we are neglecting any possible interactions between nuclei. This is a fair

approximation for amorphous targets and a good first approximation for crystalline targets also.

Case 1: High-energy elastic collisions, $\rho \ll a$.

Rutherford scattering describes this type of interaction accurately. Recall that for simple Coulomb scattering, the energy transfer cross section [Eq. (1.102)] is as follows:

$$\sigma_{\mathrm{s}}(E_{\mathrm{i}}, T) = \frac{\pi b_0^2}{4}\frac{\gamma E_{\mathrm{i}}}{T^2}.$$

Therefore, the stopping power becomes:

$$\begin{aligned}\left.\frac{\mathrm{d}E}{\mathrm{d}x}\right|_{\mathrm{n}} &= NS_{\mathrm{n}}(E_{\mathrm{i}}) = N\int_{\check{T}}^{\gamma E_{\mathrm{i}}} T\frac{\pi b_0^2}{4}\frac{\gamma E_{\mathrm{i}}}{T^2}\mathrm{d}T \\ &= \frac{N\pi b_0^2}{4}\gamma E_{\mathrm{i}}\ln\left(\frac{\gamma E_{\mathrm{i}}}{\check{T}}\right),\end{aligned} \tag{1.130}$$

where $\hat{T} = \gamma E_{\mathrm{i}}$ and $\check{T}$ is the value of T which yields $b = a$ or $\check{T}_b = \dfrac{e^2\gamma E_a^2}{4E_{\mathrm{i}}}$.

Substituting for b_0 from Eq. (1.93) gives:

$$\left.\frac{\mathrm{d}E}{\mathrm{d}x}\right|_{\mathrm{n}} = NS_{\mathrm{n}}(E_{\mathrm{i}}) = \frac{N\pi Z_1^2 Z_2^2 \varepsilon^4}{E_{\mathrm{i}}}\frac{M_1}{M_2}\ln\left(\frac{\gamma E_{\mathrm{i}}}{\check{T}_b}\right). \tag{1.131}$$

Note that for like atoms, $\gamma = 1$ and $M_1 = M_2$, so:

$$NS_{\mathrm{n}}(E_{\mathrm{i}}) = \frac{N\pi Z_1^2 Z_2^2 \varepsilon^4}{E_{\mathrm{i}}}\ln\left(\frac{E_{\mathrm{i}}}{\check{T}_b}\right). \tag{1.132}$$

Substituting for E_a from Eq. (1.107) into the expression for $\check{T}_b$ gives:

$$\check{T}_b = \frac{4E_{\mathrm{R}}^2(Z_1Z_2)^2(Z_1Z_2)^{2/6}}{\mathrm{c}^2 E_{\mathrm{i}}}. \tag{1.133}$$

Using $a = a_0/(Z_1Z_2)^{1/6}$ and substituting for $(Z_1Z_2)^{1/6}$ gives:

$$\check{T}_b = \frac{4E_{\mathrm{R}}^2 a_0^2 Z^4}{\mathrm{c}^2 a^2 E_{\mathrm{i}}},$$

for $Z_1 = Z_2$, and since $\varepsilon^2 = 2a_0E_R$, then Eq. (1.132) becomes:

$$\begin{aligned} NS_n(E_i) &= \frac{4N\pi Z^4 a_0^2 E_R^2}{E_i} \ln\left(\frac{E_i}{\check{T}_b}\right) \\ &= \frac{4N\pi Z^4 a_0^2 E_R^2}{E_i} \ln\left(\frac{c^2 a^2 E_i^2}{4a_0^2 E_R^2 Z^4}\right). \end{aligned} \tag{1.134}$$

Case 2: Low-energy elastic collisions, $\rho \sim a$.

At intermediate and lower energies, pure Coulomb scattering will not correctly capture the interaction. Here, we must use a screened Coulomb function to account for the effects of the electrons in the internuclear space. Bohr showed that the screened Coulomb potential could be accurately described using an inverse power potential of the form [14]:

$$\sigma(E,T) = \frac{C_m}{E^m T^{1+m}}, \tag{1.135}$$

where

$$C_m = \frac{\pi}{2}\lambda_m a^2 \left(\frac{2Z_1 Z_2 \varepsilon^2}{a}\right)^{2m} \left(\frac{M_1}{M_2}\right)^m, \tag{1.136}$$

and λ_m is a fitting variable. Inserting the potential function in Eq. (1.135) into Eq. (1.129) for the stopping power gives:

$$S_n(E) = \frac{1}{N}\left(\frac{dE}{dx}\right)_n = \frac{C_m}{E^m}\int_0^{\hat{T}} T^{-m} dT = \frac{C_m E^{-m} T^{1-m}}{1-m}\Bigg|_0^{\hat{T}}, \tag{1.137}$$

$$S_n(E) = \frac{C_m E^{1-2m}}{1-m}\gamma^{1-m}, \tag{1.138}$$

where γ has the usual definition, Eq. (1.14). Lindhard et al. [14] introduced a set of dimensionless or reduced variables for energy, $\in$, and distance, ρ_x:

$$\in = \frac{M_2}{(M_1+M_2)}\frac{a}{Z_1 Z_2 \varepsilon^2}E, \tag{1.139}$$

$$\rho_x = N4\pi a^2 \frac{M_1 M_2}{(M_1+M_2)^2}x. \tag{1.140}$$

They proposed a universal, one-parameter, differential scattering cross section in reduced notation that approximates the interaction potential $V(r) = \dfrac{Z_1 Z_2 \varepsilon^2}{r}\phi_0(r/a)$, where ϕ_0 is the Fermi function belonging to a single Thomas–Fermi atom:

$$\sigma = \frac{\pi a^2}{2}\frac{f(t^{1/2})}{t^{3/2}}, \tag{1.141}$$

where t is a dimensionless collision parameter defined by:

$$t = \in^2 \frac{T}{\hat{T}} = \frac{1}{2}\in^2 (1 - \cos\phi) = \in^2 \sin^2 \phi/2, \tag{1.142}$$

and t is proportional to the energy transfer, T, and to the energy, E_i, through $\in^2 /\hat{T}$, and ϕ is the CM scattering angle. Lindhard et al. [14] treated $f(t^{1/2})$ to be a simple scaling function where t was a measure of the depth of penetration into an atom during a collision and large t represents close approach. The function $f(t^{1/2})$ is plotted in Fig. 1.17, and Winterbon et al. [15] developed an analytical expression for the function:

$$f(t^{1/2}) = \lambda' t^{1/6}\left[1 + (2\lambda' t^{2/3})^{2/3}\right]^{-3/2}, \tag{1.143}$$

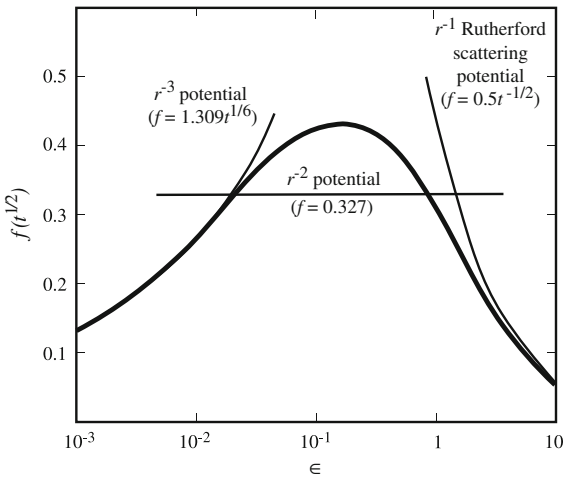

Fig. 1.17 Reduced differential cross section calculated from the Thomas–Fermi potential. Abscissa is $\in = t^{1/2}/\sin\phi/2$. The *thick solid line* ranging over $10^{-3} < \in < 10$ is from Eq. (1.141). The *thin solid lines* at *left* and *right* and the *horizontal line* in the *middle* are calculated using the power law cross section, Eq. (1.144) (after [15])

where $\lambda' = 1.309$. A generalization of Eq. (1.143) for power law scattering is as follows:

$$f(t^{1/2}) = \lambda_m t^{\frac{1}{2}-m}, \tag{1.144}$$

where $\lambda_{1/3} = 1.309$, $\lambda_{1/2} = 0.327$, and $\lambda_1 = 0.5$. Equation (1.144) approximately describes scattering from a potential of the form $V(r) \propto r^{-s} = r^{-1/m}$, where s is the power law exponent. At low energies (low $\in$), there is little penetration in the collision (t is small) and collisions are described by a power law with $V(r) \propto r^{-3}$ and $m = 1/3$, yielding a $t^{1/6}$ dependence. At higher energies, screening effects are minimal and are described by a $V(r) \propto r^{-1}$ potential and $m = 1$, giving $t^{-1/2}$ behavior. At intermediate energies, the function (cross section) is slowly varying and is best described by a power law potential for the form, $V(r) \propto r^{-2}$, with $m = 1/2$ giving no dependence on t, which means that the cross section is independent of $\in$. For the case of the inverse square law, $m = 1/2$ and the stopping power is given by Eq. (1.138):

$$S_n(E) = 4\pi\lambda_{1/2} a Z_1 Z_2 \varepsilon^2 \frac{M_1}{M_1 + M_2}. \tag{1.145}$$

The reduced stopping cross section, $S_n(\in)$, is given as follows:

$$S(\in) = \frac{d \in}{d\rho_x}, \tag{1.146}$$

and a relation between $S_n(E)$ and $S_n(\in)$ is as follows:

$$\frac{d \in}{d\rho_x} = \left(\frac{d \in}{dE}\frac{d\rho_x}{dx}\right)\frac{dE}{dx}. \tag{1.147}$$

Taking differentials of $\in$ with respect to E (Eq. (1.139)), and ρ_x with respect to x (Eq. (1.140)) gives:

$$S_n(\in) = \frac{M_1 + M_2}{M_1}\frac{1}{4\pi a Z_1 Z_2 \varepsilon^2} S_n(E) \tag{1.148}$$

$$= \frac{\in}{\pi a^2 \gamma E_i} S_n(E). \tag{1.149}$$

Substituting the expression for $S_n(E)$ from Eq. (1.145) into Eq. (1.148) gives:

$$S_n(\in) = \lambda_{1/2} = 0.327. \tag{1.150}$$

The stopping power can also be written using the energy transfer cross section in reduced notation from Eq. (1.141) giving:

$$S_{\mathrm{n}}(E) = \frac{1}{N}\left(\frac{\mathrm{d}E}{\mathrm{d}x}\right)_{\mathrm{n}} = \pi a^2 \int_0^{\hat{T}} T \frac{f(t^{1/2})}{2t^{3/2}}\,\mathrm{d}t = \frac{-\pi a^2 \hat{T}}{\in^2} \int_0^{\hat{T}} f(t^{1/2})\mathrm{d}t^{1/2}. \tag{1.151}$$

Substituting the stopping power $S_{\mathrm{n}}(E)$ in Eq. (1.151) into Eq. (1.149) for $\hat{T} = \gamma E_{\mathrm{i}}$ gives:

$$S_{\mathrm{n}}(\in) = \frac{1}{\in} \int_0^{\in} f(t^{1/2})\mathrm{d}t^{1/2}. \tag{1.152}$$

Setting $y = t^{1/2}$ in Eq. (1.144), Eq. (1.152) becomes:

$$S_{\mathrm{n}}(\in) = \frac{\lambda_m}{\in} \int_0^{\in} y^{1-2m} dy = \frac{\lambda_m}{\in} \frac{y^{2-2m}}{2(1-m)}\bigg|_0^{\in} = \frac{\lambda_m}{2(1-m)} \in^{1-2m}, \tag{1.153}$$

which is the power law approximation to the reduced nuclear stopping cross section. For the case of the inverse square law, $m = 1/2$ and $S_{\mathrm{n}}(\in) = \lambda_{1/2} = 0.327$.

Two approximations for $S_{\mathrm{n}}(E_{\mathrm{i}})$ for collisions in the intermediate energy regime are considered. The first is obtained by solving the orbital Eq. (1.76) using the inverse square potential in Eq. (1.59) [16]:

$$\frac{\phi}{\pi} = 1 - \frac{1}{\left(1 + \dfrac{a^2 E_a}{b^2 E_{\mathrm{i}}}\right)^{1/2}}.$$

Using Eq. (1.14) to determine T gives:

$$T = \gamma E_{\mathrm{i}} \cos^2 \left[\frac{\pi}{2}\left(1 + \frac{a^2 E_a}{b^2 E_{\mathrm{i}}}\right)^{1/2}\right]. \tag{1.154}$$

Expressing b^2 in terms of T and differentiating, and using the relation between $\sigma_{\mathrm{s}}(E_{\mathrm{i}}, T)$ and b from Eq. (1.78) gives:

$$\sigma_{\mathrm{s}}\left(E_{\mathrm{i}}, T\right) = \frac{4 E_a a^2 \alpha}{\gamma E_{\mathrm{i}}^2 \left(1 - 4\alpha^2\right)^2 \left(x(1-x)\right)^{1/2}}, \tag{1.155}$$

where $x = T/E_i$, $\pi\alpha = \cos^{-1}\sqrt{x}$, and for small x, Eq. (1.155) has the form:

$$\sigma_s\left(E_i, T\right) = \frac{\pi^2 a^2 E_a \gamma^{1/2}}{8 E_i^{1/2} T^{3/2}}. \tag{1.156}$$

The total cross section and mean recoil energy are calculated from Eq. (1.156) taking a cutoff to zero at $\overline{T} = \gamma E_i$:

$$\overline{T} = \left(\gamma E_i \check{T}\right)^{1/2}, \tag{1.157}$$

$$\sigma_s\left(E_i\right) = \frac{\pi^2 a^2 E_a \gamma^{1/2}}{4\left(E_i \check{T}\right)^{1/2}}. \tag{1.158}$$

The stopping power is determined using:

$$S_n(E_i) = \int_{\check{T}}^{\hat{T}} T\sigma(E_i, T)dT,$$

and substituting the energy transfer cross section from Eq. (1.158) yields:

$$S_n\left(E_i\right) = \frac{1}{N}\left(\frac{dE}{dx}\right)_n = \frac{\pi^2}{4} a^2 E_a \gamma. \tag{1.159}$$

Substitution for E_a from Eq. (1.107) gives a value of 0.327 for S_n. This same result can be obtained using the expression for average energy loss:

$$\frac{dE}{dx} = \frac{\overline{T}}{\lambda} = N\sigma_s \overline{T}, \tag{1.160}$$

where $\lambda = \dfrac{1}{N\sigma_s}$ is the mean free path between collisions, and substituting for $\sigma_s(E_i)$ and $\overline{T}$ from Eqs. (1.157) and (1.158).

The second approximation of $S_n(E_i)$ can be obtained using the Thomas–Fermi screening function. We will assume that a series of small-angle scattering events are responsible for most of the energy loss of a projectile in a target. When this is true, the energy transferred, T, can be expressed as a function of E_i and b by solving Eq. (1.76) for ϕ using the Thomas–Fermi screening function, Eq. (1.49), and expanding the solution on the assumption that f is small. Proceeding, we find:

$$\phi = \pi - 2\int_{\circ}^{\hat{x}} \left[\frac{1}{b^2}\left(1 - \frac{V(x)}{\eta E_i} - b^2 x^2\right)\right]^{-1/2} dx, \tag{1.161}$$

and for $V(r) = \dfrac{Z_1 Z_2 \varepsilon^2}{r} f(r/a)$, where $f(r/a) = a/r$, the solution is as follows:

$$\phi = \pi - b\left[b^2 + \frac{Z_1 Z_2 \varepsilon^2 a}{E_R}\right]^{-1/2}. \tag{1.162}$$

Solving for b and substituting in the expression:

$$\sigma_s\left(E_i, \phi\right)\, \mathrm{d}\Omega = 2\pi b\, \mathrm{d}b,$$

and using Eq. (1.15) to obtain $\sigma_s(E_i, T)\, dT$, we can then find $S_n(E_i)$ from Eq. (1.129). The result is as follows:

$$S_n^0 = \frac{\pi^2}{e}\varepsilon^2 a_0 Z_1 Z_2 \frac{M_1}{M_1 + M_2} Z^{-1/3}, \tag{1.163}$$

which is the standard stopping power and is shown in Fig. 1.18. Note that S_n^0 is independent of the projectile energy to a first approximation, and substitution of Eqs. (1.163) and (1.139) into Eq. (1.149) yields a value of 0.327 for S_n^0. Ranges estimated from S_n^0 will be reasonably close when small-angle scattering predominates.

Recall that the key assumption in deriving Eq. (1.163) was that energy loss of a projectile can be represented as a series of small-angle scattering events, allowing us to then assume that f remains small. Table 1.6 gives the scattering angles and energy loss for a 50 keV silicon projectile incident on a silicon target atom. Note that for $\rho/a \geq 1$, this assumption is clearly valid.

The nuclear stopping cross section in reduced notation is determined by using Eq. (1.149) for $S_n(\in)$ and substituting Eq. (1.129) for $S_n(E)$ giving:

$$S_n(\in) = \frac{\in}{\pi a_U^2 \gamma E_i} \int_0^{\hat{T}} T\sigma_s(E_i, T)\mathrm{d}T, \tag{1.164}$$

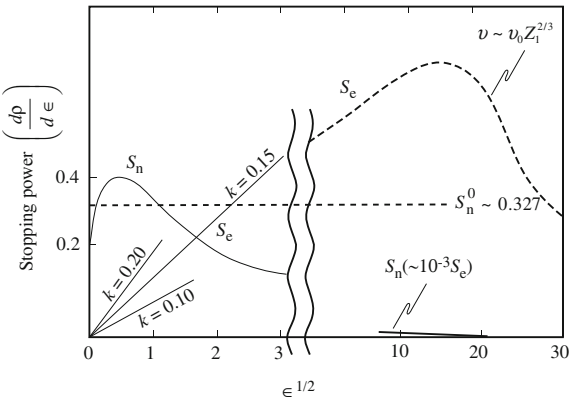

Fig. 1.18 The reduced nuclear and electronic stopping cross sections as a function of $\in^{1/2}$

Table 1.6 Scattering angles and energy loss for a 50 keV silicon projectile and a silicon target atom [17]

ρ/a =	10	1	0.1
ϕ (radians)	0.004π	0.26π	0.89π
θ (degrees)	0.36	23.4	80.5
T/E	4×10^{-5}	0.16	0.973
T (keV)	0.002	8	49

where the universal screening length a_U is substituted for the Thomas–Fermi screening length a, and using the identity:

$$\int_0^{\hat{T}} \sigma_s(E_i, T)\mathrm{d}T = \int_0^{b_{\max}} 2\pi b \mathrm{d}b, \tag{1.165}$$

yields an expression for the nuclear stopping cross section in reduced notation:

$$S_n(\in) = \frac{\in}{a_U^2} \int_0^{\infty} \sin^2 \frac{\phi}{2} \mathrm{d}b^2. \tag{1.166}$$

Ziegler [18] used the universal screening function, Fig. 1.19:

$$\chi_U = 0.1818e^{-3.2x} + 0.5099e^{-0.9423x} + 0.2802e^{-0.4028x} + 0.02817e^{-0.2016}, \tag{1.167}$$

and the numerical integration of Eq. (1.76) and Eq. (1.166) to calculate a universal reduced nuclear stopping cross section, the ZBL cross section shown in Fig. 1.20. An expression for the fit is as follows:

$$S_n(\in) = \frac{0.5 \ln(1 + 1.1383 \in)}{(\in + 0.01321 \in^{0.21226} + 0.19593 \in^{0.5})}, \tag{1.168}$$

and for practical calculations, the ZBL universal nuclear stopping for an ion with energy E_i in the laboratory system is as follows:

$$S_n(E_i) = \frac{8.462 \times 10^{-15} Z_1 Z_2 M_1 S_n(\in)}{(M_1 + M_2)(Z_1^{0.23} + Z_2^{0.23})} \frac{\mathrm{eV} \cdot \mathrm{cm}^2}{\mathrm{atom}}, \tag{1.169}$$

where the ZBL reduced energy is as follows:

$$\in = \frac{32.53 M_2 E_i}{Z_1 Z_2 (M_1 + M_2)(Z_1^{0.23} + Z_2^{0.23})}. \tag{1.170}$$

Let us now look at electronic energy loss.

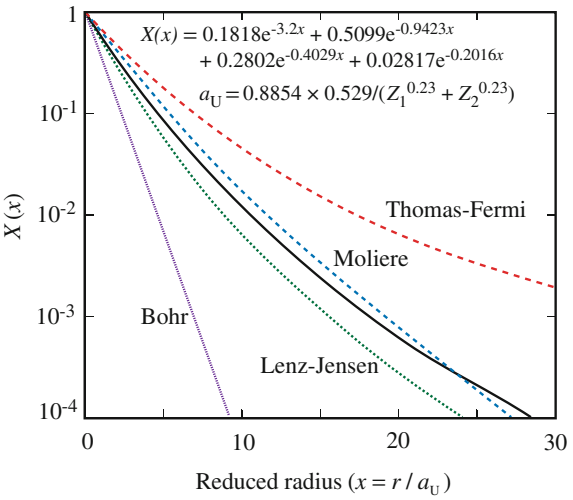

Fig. 1.19 The universal screening function χ_U (*solid thick line*) from Eq. (1.167) as a function of $x = r/a_{U,}$ where a_U is the universal screening length defined by $a_U = 0.8854a_0/(Z_1^{0.23} + Z_2^{0.23})$, along with several other screening functions (after [19])

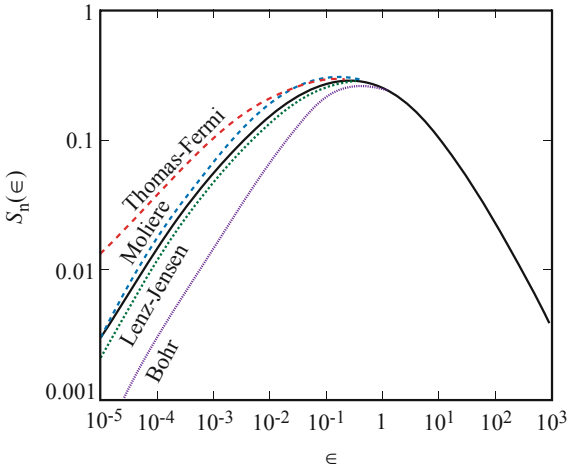

Fig. 1.20 Nuclear stopping power in reduced units from Eq. (1.168)

Electronic Stopping Power

The theoretical computation of electronic stopping power is a much more complicated problem than the calculation of S_n. For the description of collisions between ions and electrons, we may use the classical equation (Eq. (1.106)). But here we must consider that the binary collision is between a heavy moving ion and an electron in a solid. This approach is valid as long as all electrons participate and the ion velocity exceeds the velocity of the tightest bound electron. We may define T by:

$$\hat{T} \cong \gamma_e E_i, \tag{1.171}$$

where $\gamma_e = \dfrac{4m_e M}{(m_e + M)^2}$, and hence, $\hat{T}$ is very small. We will also define a lower limit for ion–electron interactions as the effective mean excitation–ionization level $\bar{I}$.[1] We also note that we must use the electron density, which is just Z_2 times the atom density:

$$n = NZ_2. \tag{1.172}$$

Writing an expression for stopping power due to excitation–ionization interactions that is equivalent to Eq. (1.130) yields:

$$\begin{aligned}\left(-\frac{dE}{dx}\right)_e &= \frac{n}{Z_2}\int_{\bar{I}}^{\gamma_e E_i} T\sigma_s(E_i, T)\,dT \\ &= \frac{n}{Z_2}\frac{\pi b_0^2}{4}\gamma_e E_i \ln\left(\frac{\gamma_e E_i}{\bar{I}}\right) \\ &= N\pi\frac{Z_1^2 Z_2 \varepsilon^4}{E_i}\frac{M}{m_e}\ln\left(\frac{\gamma_e E_i}{\bar{I}}\right).\end{aligned} \tag{1.173}$$

This formula is only approximate. A more exact expression is obtained from a quantum mechanical treatment based on the Born approximation, which is interpreted physically to mean that the perturbation due to the incident particle does not seriously disturb the electronic motion for large impact parameters. The result of this analysis is the addition of a factor of 2, which comes from the small-energy transfer processes where free Coulomb scattering is invalid. The Bethe–Bloch formula is a good approximation:

$$\left(-\frac{dE}{dx}\right)_e = \frac{2N\pi Z_1^2 Z_2 \varepsilon^4}{E_i}\frac{M}{m_e}\ln\left(\frac{\gamma_e E_i}{\bar{I}}\right) = \frac{2\pi N Z_1^2 M \varepsilon^4}{m_e E_i}B, \tag{1.174}$$

where $B = Z_2 \ln\left(\dfrac{\gamma_e E_i}{\bar{I}}\right)$ is the stopping number. For relativistic velocities:

$$B = Z_2\left\{\ln\left(\frac{\gamma_e E_i}{\bar{I}}\right) - \ln(1-\beta^2) - \beta^2\right\}, \tag{1.175}$$

where $\beta = \upsilon/c$ and c is the speed of light. Note that at high energies, S_n and S_e vary as $1/E_i$ very nearly, and:

$$\frac{S_e}{S_n} = \frac{2M_2}{m_e Z_2}\frac{\ln\left(\dfrac{\gamma_e E_i}{\bar{I}}\right)}{\ln\left(\dfrac{\gamma E_i}{E_d}\right)}. \tag{1.176}$$

[1] To a first approximation, $\bar{I} = kZ_2$ where $k = 11.5$ eV.

Applying Eq. (1.176) to the case of MeV protons, the value is ~2000 for $\bar{I} \sim 11.5Z_2$ eV, or the electronic stopping power is 2000 times that of the nuclear stopping power.

At low velocities, electrons in the inner shells contribute less to the stopping power. Also, the neutralization probability becomes so large that the collision between the projectiles and the surrounding electrons is almost elastic. The energy loss becomes proportional to the projectile velocity. Lindhard, Scharff, Schiott (LSS), and Firsov gave theoretical descriptions for this energy region. The LSS expression is based on elastic scattering of free target electrons in the static field of a screened point charge. Firsov's is based on a simple geometric model of momentum exchange between the projectile and target atom during interpenetration of electron clouds. Lindhard and Winther [17] have shown that as long as the ion velocity is less than the velocity of an electron having an energy equal to the Fermi energy, E_f of the free electron gas, S_e will be proportional to the velocity of the ion or the one-half power of its energy. Using a potential of the form:

$$V(r) = \frac{2(Z_1 Z_2)^{1/2}\varepsilon^2}{r}\chi_{TF}\left[1.13\left(Z_1^{2/3} + Z_2^{2/3}\right)^{1/2}\frac{r}{a_0}\right], \tag{1.177}$$

the Lindhard–Scharff stopping power becomes:

$$S_e(E) = \left(-\frac{dE}{dx}\right)_e \frac{1}{N} = k' E^{1/2}, \tag{1.178}$$

$$k' = 3.83\frac{Z_1^{7/6} Z_2}{M_1^{1/2}\left(Z_1^{2/3} + Z_2^{2/3}\right)^{3/2}}, \tag{1.179}$$

where $S_e(E)$ is given in units of 10^{-15} eV cm^2/atom and E is in keV. Expressing the stopping cross section in reduced notation gives:

$$S_e(\in) = \left(\frac{d\in}{d\rho}\right)_e = k\in^{1/2}, \text{ where}$$
$$k = \frac{0.07937 Z_1^{2/3} Z_2^{1/2}\left(1 + \frac{M_2}{M_1}\right)^{3/2}}{\left(Z_1^{2/3} Z_2^{2/3}\right)^{3/4} M_2^{1/2}}. \tag{1.180}$$

The universal nuclear stopping cross section is shown in Fig. 1.18 where a single curve represents all possible projectile–atom collisions, and the electronic stopping cross section of Eq. (1.180) results in a family of lines or one for each combination of projectile and target atom.

An approximate treatment that results in an analytical expression is obtained in the following analysis. Consider an atom of mass M_1, moving with velocity v_1,

which makes a head-on collision with an electron moving in the opposite direction with velocity υ_e. The relative initial speed of the two particles is as follows:

$$\upsilon_{r0} = \upsilon_1 + \upsilon_e. \tag{1.181}$$

After collision, the velocity vector changes but not the magnitude:

$$\upsilon_{rf} = -(\upsilon_1 + \upsilon_e). \tag{1.182}$$

The speed of the atom following the collision with the electron is given by:

$$\begin{aligned} \upsilon_{1f} &= V_{CM} + \left(\frac{m_e}{M_1 + m_e}\right)\upsilon_{rf} \\ &= \frac{M_1\upsilon_1 - m_e\upsilon_e}{M_1 + m_e} - \left(\frac{m_e}{M_1 + m_e}\right)(\upsilon_1 + \upsilon_e) \\ &\cong \upsilon_1 - \frac{2m_e\upsilon_e}{M_1}, \end{aligned} \tag{1.183}$$

where m_e is neglected compared to M_1. The change in the energy of the atom due to the collision is as follows:

$$\Delta E = \Delta\left(\frac{1}{2}M_1\upsilon_1^2\right) \cong M_1\upsilon_1(\upsilon_1 - \upsilon_{1f}) = 2M_e\upsilon_e\upsilon_1. \tag{1.184}$$

The electron velocity after the collision is given as follows:

$$\begin{aligned} \upsilon_{ef} &= V_{CM} - \left(\frac{m_1}{M_1 + m_e}\right)\upsilon_{rf} \\ &= \frac{M_1\upsilon_1 - m_e\upsilon_e}{M_1 + m_e} + \left(\frac{M_1}{M_1 + m_e}\right)(\upsilon_1 + \upsilon_e) = 2\upsilon_1 + \upsilon_e, \end{aligned} \tag{1.185}$$

or the increase in the electron velocity is as follows:

$$\Delta\upsilon_e = \upsilon_{ef} - \upsilon_e = 2\upsilon_1. \tag{1.186}$$

The number of conduction electrons in a metal is approximately equal to the atom number density N. But only those electrons with velocities lying in the range $\Delta\upsilon_e$ of the Fermi velocity υ_f are able to participate in the slowing down process. Therefore, the effective density of electrons in the metal is as follows:

$$n_e \cong N\left(\frac{\Delta\upsilon_e/2}{\upsilon_f}\right) = \left(\frac{\upsilon_1}{\upsilon_f}\right)N. \tag{1.187}$$

The current of effective electrons impinging on the atom is as follows:

$$I_e = n_e v_{r0} = n_e(v_1 + v_e) \cong n_e v_e, \tag{1.188}$$

and the collision rate of effective electrons with a single atom is $\sigma_e I_e$, where σ_e is the cross section for interaction of the moving atom with conduction electrons. The stopping power is then the energy loss rate of a moving atom to effective electrons divided by the velocity of the atom:

$$\left(-\frac{dE}{dx}\right)_e = \frac{\sigma_e I_e \Delta E}{v_1}. \tag{1.189}$$

Substituting Eqs. (1.184), (1.187), and (1.188) into the above expression and writing v_e and v_1 as $(2E_f/m_e)^{1/2}$ and $(2E/M_1)^{1/2}$, respectively, yield:

$$\left(-\frac{dE}{dx}\right)_e = 8\sigma_e N\left(\frac{m_e}{M_1}\right)^{1/2} E^{1/2} = kE^{1/2}, \tag{1.190}$$

where

$$k = 8\sigma_e N\left(\frac{m_e}{M_1}\right)^{1/2}, \tag{1.191}$$

and $k = 3.0NZ^{2/3}\text{eV}^{1/2}/\text{nm}$ for like atoms, or $S_e = k'E^{1/2}$ where $k' = 3 \times 10^{-15}Z^{2/3}\ \text{eV}^{1/2}\ \text{cm}^2$ for like atoms. Both equations are valid for $0 < E\ (\text{keV}) < 37Z^{7/3}$. For example, for $M_2 = \text{Si}$, $k'_{\text{Si}} \sim 0.2 \times 10^{-15}\text{eV}^{1/2}\,\text{cm}^2$. Table 1.7 summarizes the nuclear and electronic energy loss rates for the various types of interactions used in Sect. 1.3.1.

1.3.2 Range Calculations

We have developed expressions for the two major forms of energy loss: (1) collisions of the ion with the target nuclei and (2) interactions of the ion with the electrons in the solid. We will assume that these two forms of energy loss are independent of each other. Because of this approximation, we may write the total energy loss of a single projectile as the sum of the individual contributions:

$$\left(-\frac{dE}{dx}\right)_T = NS_T = N[S_n(E) + S_e(E)]. \tag{1.192}$$

This expression can be integrated to give the total distance R that a projectile of initial energy E_i will travel before coming to rest:

Table 1.7 Summary of energy loss rates for various types of interactions

Type of interaction	Nuclear energy loss rate $\left(-\frac{dE}{dx}\right)_n$		Electronic energy loss rate $\left(-\frac{dE}{dx}\right)_e$	
High E Coulomb	$\frac{4N\pi Z^4 a_0^2 E_R^2}{E_i}\ln\left(\frac{a^2c^2E_i^2}{4a_0^2E_R^2Z^4}\right)$	(1.134)	$N\pi\frac{Z_1^2Z_2e^4}{E_i}\frac{M}{m_e}\ln\left(\frac{\gamma_e E_i}{\bar{I}}\right)$	(1.173)
Low E	General expression: $\frac{8.462\times10^{-15}NZ_1Z_2M_1S_n(\in)}{(M_1+M_2)(Z_1^{0.23}+Z_2^{0.23})}$	(1.169)	$k'E_i^{1/2}$ $k' = 3.83\frac{Z_1^{7/6}Z_2}{M_1^{1/2}\left(Z_1^{2/3}+Z_2^{2/3}\right)^{3/2}}$	(1.178) (1.179)
	Inverse square: $\frac{\pi^2}{4}a^2NE_a\gamma$	(1.159)	$kE_i^{1/2}$	(1.190)
	Thomas–Fermi screening: $K\frac{NZ_1Z_2}{Z^{1/3}}\frac{M_1}{M_1+M_2}$ where $Z^{1/3} = \left(Z_1^{2/3}+Z_2^{2/3}\right)^{1/2}$ and $K = \left(\frac{\pi}{e}\right)\varepsilon^2 a_0 = 2.8\times10^{-15}\,\text{eV}\cdot\text{cm}^2$	(1.163)	$k = 8\sigma_e N\left(\frac{m_e}{M_1}\right)^{1/2}$ valid for $0 < E\,(\text{keV}) < 37Z^{7/3}$	

$$R = \int_0^R dx = \frac{1}{N}\int_0^{E_i}\frac{dE}{[S_n(E)+S_e(E)]}. \tag{1.193}$$

This distance is called the average total range and is a useful quantity for making estimates of the average penetration depths of ions in amorphous targets. In general, the total path length due only to nuclear stopping can be obtained by substituting the nuclear stopping power from Eq. (1.138) into:

$$R = \int_0^{E_i}\frac{dE}{NS_n(E)}\frac{\pi}{2}, \tag{1.194}$$

to give:

$$R(E_i) = \left(\frac{1-m}{2m}\right)\frac{\gamma^{m-1}}{NC_m}E_i^{2m}, \tag{1.195}$$

and in reduced notation, substituting the stopping power given in Eq. (1.153) into:

$$\rho_x = \int_0^{\in}\frac{d\in}{S_n(\in)}, \tag{1.196}$$

to give:

$$\rho_x = \frac{1-m}{m\lambda_m} \in^{2m} . \tag{1.197}$$

An estimate of the total path length for the case of nuclear stopping only with application of the inverse square potential [see Eq. (1.156)] is as follows:

$$\begin{aligned} \frac{\mathrm{d}E}{\mathrm{d}x} &= N \int_{\check{T}}^{\gamma E_\mathrm{i}} T\sigma_\mathrm{s}(E_\mathrm{i}, T)\mathrm{d}T \quad \text{where} \quad \sigma_\mathrm{s}(E_\mathrm{i}, T) = \frac{\pi^2 a^2 E_a \gamma^{1/2}}{8E_\mathrm{i}^{1/2} T^{3/2}} \\ &= \frac{\pi^2}{4} a^2 N E_a \gamma, \end{aligned} \tag{1.198}$$

so,

$$\begin{aligned} \overline{x} = \overline{R}_\mathrm{total} &= \int_0^{E_\mathrm{i}} \frac{\mathrm{d}E'}{(\mathrm{d}E/\mathrm{d}x)_n} = \int_0^{E_\mathrm{i}} \frac{\mathrm{d}E'}{\frac{\pi^2}{4} a^2 N E_a \gamma} \\ &\frac{4E_\mathrm{i}}{\pi^2 a^2 N E_a \gamma} \quad \text{where} \quad E_\mathrm{i} \leq E_a. \end{aligned} \tag{1.199}$$

The quantity of interest is, however, the projection of the total range on the initial direction of the particle path (Fig. 1.21). In addition, we want to know the deviation in the projected range, which arises from the fact that all particles do not suffer the same sequence of collisions. We then define:

$\overline{R_\mathrm{p}} \equiv$ mean projected range and

$\overline{\Delta R_\mathrm{p}} \equiv$ standard deviation of the projected range.

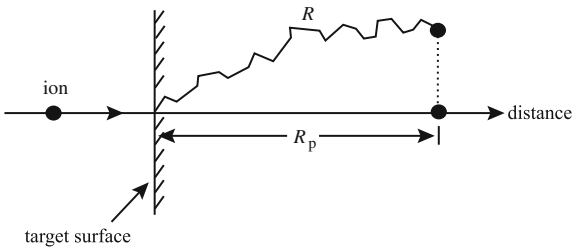

Fig. 1.21 Total path length R and projected range R_p for an ion incident on a target

Methods for computing $\overline{R_\mathrm{p}}$ have been developed by Lindhard et al. [16]. In cases where the energy transfer T is small compared to the total energy of the particle, the differential equation for $\overline{R_\mathrm{p}}$ has the solution:

$$\overline{R_\mathrm{p}} = \int_0^{E_\mathrm{i}} \frac{\mathrm{d}E'}{\beta_1(E')} \exp\left[\int_{E_\mathrm{i}}^{E'} \frac{\alpha_1(x)\,\mathrm{d}x}{\beta_1(x)}\right], \tag{1.200}$$

where $\alpha_1(E) = \dfrac{\mu}{2} N \dfrac{S_\mathrm{n}(E)}{E}$,

$$\beta_1(E) = N\left[S_\mathrm{n}(E) + S_\mathrm{e}(E) - \frac{\mu}{2}\frac{\Omega_\mathrm{n}^2(E)}{E}\right], \tag{1.201}$$

and $\Omega_\mathrm{n}^2(E) = \int_0^\infty T_\mathrm{n}^2 2\pi b\,\mathrm{d}b$.

The standard deviation is computed by defining the quantities R_c (chord range) and $R_\perp$ (range perpendicular to the initial direction) so that, from Fig. 1.22, we have the following relation:

$$\overline{R_\mathrm{c}^2} = \overline{R_\mathrm{p}^2} + \overline{R_\perp^2}, \tag{1.202}$$

and a related quantity:

$$\overline{R_\mathrm{r}^2} = \overline{R_\mathrm{p}^2} - \frac{1}{2}\overline{R_\perp^2}, \tag{1.203}$$

and for cases where $T \ll E$:

$$\overline{R_\mathrm{r}^2(E)} = \int_0^E \frac{2\overline{R_\mathrm{p}(E')}\,\mathrm{d}E'}{\beta_2(E')} \exp\left[\int_E^{E'} \frac{3\alpha_2(x)}{\beta_2(x)}\mathrm{d}x\right], \tag{1.204}$$

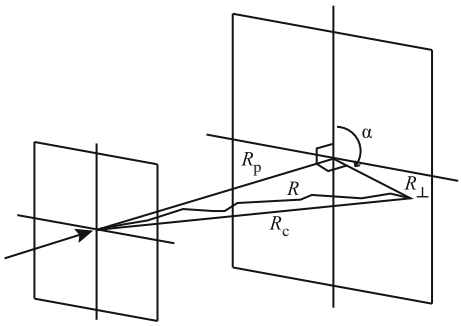

Fig. 1.22 Schematic of the definition of range parameters R, R_p, R_c, $R_\perp$

and

$$\overline{R_c^2(E)} = \int_0^E \frac{2\overline{R_p(E')}\,dE'}{N[S_n(E') + S_e(E')]}, \tag{1.205}$$

and then $\overline{\Delta R_p}$ is found from:

$$(\overline{\Delta R_p})^2 = \frac{2\overline{R_r^2}(E) + \overline{R_c^2}(E)}{3} - (\overline{R_p})^2, \tag{1.206}$$

where $\alpha_2(E) = \alpha_1(E)/2, \beta_2(E) = \beta_1(E) - \dfrac{N\mu\Omega_n^2(E)}{E}$.

The integrals can be evaluated numerically for the Thomas–Fermi potential or analytically if the approximate values of S_n and S_e are used together with the value:

$$\Omega_n^2(E) = \frac{4M_1M_2}{3(M_1 + M_2)} S_n^0 E. \tag{1.207}$$

In LSS formalism, the average total path length can be calculated from:

$$\rho_R = \int_0^{\in} \frac{d \in}{[S_n(\in) + S_e(\in)]} = \int_0^{\in} \frac{d \in}{[S_n(\in) + k \in^{1/2}]}. \tag{1.208}$$

This expression must be integrated numerically using different values of k. For a particular Z_1, Z_2, and E_i, we calculate $\in$ and k and then read off the value of ρ_R from Fig. 1.23 and convert to R using Eqs. (1.139), (1.140), and $\rho_R = 3.06\varepsilon$:

$$R(\text{nm}) = \frac{6EM_2(M_1 + M_2)\left(Z_1^{2/3} + Z_2^{2/3}\right)^{1/2}}{\rho Z_1 Z_2 M_1}, \tag{1.209}$$

where E is in keV and ρ is in g/cm^3. The most interesting range quantity of interest is the average projected range, R_p, and this is what is usually measured. At high energies, $S_e \gg S_n$ and $R \sim R_p$. At low energies where $S_n \sim S_e$, then $R_p < R$. This difference gets larger with M_2/M_1. LSS theory also analyzed this problem.

At low $\in$ or ρ_R (and small values of k):

$$\begin{aligned} \text{For} \quad & M_2/M_1 = \frac{1}{2}; \quad R/R_p \sim 1.2 \\ & M_2/M_1 = 1; \quad R/R_p \sim 1.6 \\ \text{and} \quad & M_2/M_1 = 2; \quad R/R_p \sim 2.2. \end{aligned}$$

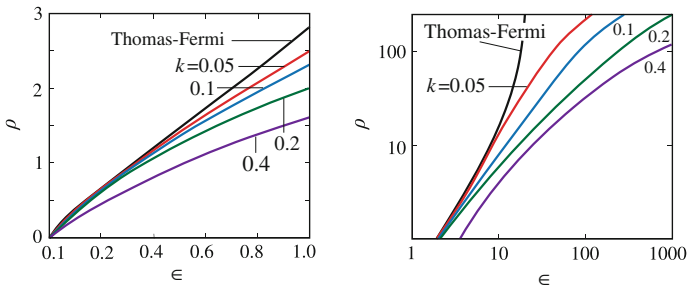

Fig. 1.23 Reduced range–energy plots for various values of the electronic stopping parameter, k

At high energies ($\in$ large), $R/R_p \rightarrow 1$ for all k. Finally as a general approximation [16]:

$$\frac{R}{R_p} \cong 1 + B\frac{M_2}{M_1}, \tag{1.210}$$

where B is a slowly varying function of E and R. In the energy region where nuclear stopping dominates and $M_1 > M_2$, $B = 1/3$. Increased electronic stopping at higher energies leads to smaller values of B. When $M_1 < M_2$, large-angle scattering increases the difference between R and R_p. However, for these collisions, electronic stopping is appreciable and partially offsets the increase in the difference. Therefore, $B = 1/3$ is a reasonable approximation for a wide range of conditions, giving:

$$R_p \cong \frac{R}{1 + (M_2/3M_1)}. \tag{1.211}$$

Range straggling can be calculated using the theory of Lindhard et al. [16]. For the case where nuclear stopping dominates and $M_1 > M_2$, i.e., small-angle scattering:

$$2.5\Delta R_p \cong 1.1R_p\left[\frac{2(M_1M_2)^{1/2}}{M_1 + M_2}\right], \tag{1.212}$$

or

$$\Delta R_p \cong R_p/2.5. \tag{1.213}$$

For a high-energy ion, the slowing down path is essentially a straight line in the original direction of motion, since the stopping is electronic with a small amount of straggle at the end due to nuclear collisions (Fig. 1.24(a)). At lower energies where S_n and S_e are more comparable, the ion path follows a zigzag course with many large deflections with the distance between collisions decreasing as the energy

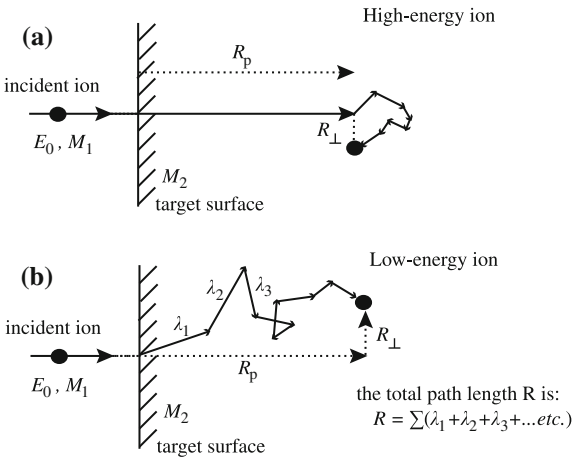

Fig. 1.24 Total path length, projected range, and perpendicular range for (**a**) high-energy ions and (**b**) low-energy ions incident on a target

decreases and the cross section increases (Fig. 1.24(b)). The incident particles are distributed according to a Gaussian as:

$$N(x) = N_p e^{-1/2X^2}, \tag{1.214}$$

where $X = \dfrac{x - R_p}{\Delta R_p}$ and ΔR_p is the standard deviation (Fig. 1.25). If the peak concentration is N_p at R_p, then this will fall to $\dfrac{1}{e^{1/2}} N_p$ at distances $x = R_p \pm \Delta R_p$. If we view the target perpendicularly through its surface, then the number of implanted ions per unit area will be N_s, given by:

$$N_s = \int_{-\infty}^{+\infty} N(x)\,\mathrm{d}x, \tag{1.215}$$

or since $\mathrm{d}x = \Delta R_p \mathrm{d}X$ and the Gaussian curve is symmetrical, then:

$$N_s = 2\Delta R_p N_p \int_0^{\infty} e^{-1/2X^2}\,\mathrm{d}X, \tag{1.216}$$

which can be written as follows:

$$N_s = \Delta R_p N_p \sqrt{2\pi} \left\{ \sqrt{\frac{2}{\pi}} \int_0^{\infty} e^{-1/2X^2}\,\mathrm{d}X \right\}. \tag{1.217}$$

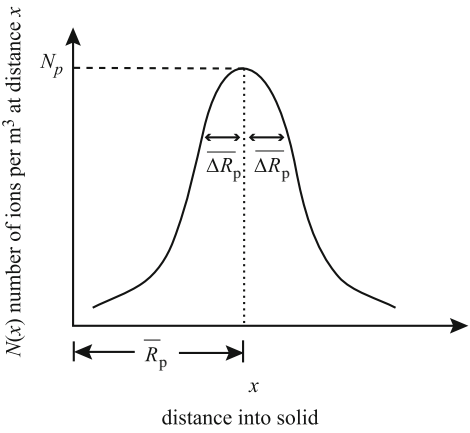

Fig. 1.25 Parameters of the Gaussian distribution applied to an ion implantation profile showing the projected range, $\overline{R}_p$, the straggling or standard deviation, $\overline{\Delta R}_p$, and the maximum concentration, N_p of the implanted ion

The integral inside the bracket is the error function and tends to unity as $X \rightarrow \infty$, so that if N_s is the number of ions/cm^2 implanted into the target, we have:

$$N_p = \frac{N_s}{\sqrt{2\pi}\Delta R_p} \cong \frac{0.4N_s}{\Delta R_p}, \tag{1.218}$$

so the density of implanted ions is as follows:

$$N(x) = \frac{0.4N_s}{\Delta R_p} \exp\left(-1/2\left\{\frac{x - R_p}{\Delta R_p}\right\}^2\right). \tag{1.219}$$

As an example, if we implant 5×10^{15} ions/cm^2 of 40 keV B into Si, then $R_p \sim 160$ nm, $\Delta R_p \sim 54$ nm, and $N_p \sim 4 \times 10^{20}$ atoms/cm^2. Note that from the properties of the Gaussian, the concentration will fall by one decade at $x \simeq R_p \pm 2\Delta R_p$ and by 2 decades at $x \simeq R_p \pm 3\Delta R_p$.

Using the LSS treatment to describe electronic and nuclear stopping, Littmark and Ziegler have solved for the ranges of atoms with atomic number between 1 and 92 in all elements [18]. For each atom serving as the target, the mean ion depth, longitudinal straggling, and transverse straggling are compiled in graphs for projectiles with $1 \leq Z \leq 92$ and over a wide energy range. The following example is taken from this handbook.

Example 1.3. MeV He implantation into Si
Zeigler [18] plots and tabulates the range parameters for a wide range of ions and target atoms. For 2 MeV He incident on a Si target, the range and straggling are 7.32 μm and 0.215 μm, respectively. If we assume a dose of 10^{15} He ions/cm^2, then applying Eq. (1.218) gives a peak concentration of $\sim 1.86 \times 10^{19}$ He atoms/cm^3 at a depth of 7.32 μm, which is approximately

620 appm. Equation (1.219) gives the distribution of deposited He atoms as follows:

$$N(x) = 1.86 \times 10^{19} \exp\left(-1/2\left\{\frac{x - 7.32}{0.215}\right\}^2\right) \text{He/cm}^3,$$

where x is in units of μm.

In addition to a tabulation of range data, Ziegler has developed a Monte Carlo-based computer program for calculating the transport of ions in matter [20]. The program is available on the Web at http://www.srim.org, and the reader is encouraged to try some examples using the SRIM simulation software. This program is downloadable at no cost to the user (subject to the terms of use posted on the site) and may be executed on your personal computer. The following example uses data taken from the SRIM program.

Example 1.4. Implantation of Al into Ni
A similar example can be worked for lower energy implantation of a heavier element such as Al, into a nickel target. In this case, we use the output of the SRIM program. Selecting 200 keV Al in Ni results in a projected range of ~135 nm with a longitudinal straggling of 44 nm. Substitution into Eq. (1.216) yields a peak concentration of 9.1×10^{19} Al/cm^3 for a dose of 10^{15} Al$^+$/cm^2. The SRIM software also yields a quantity that allows the user to determine concentration. The unit of concentration in the ion range plot is [atoms/cm^3/atoms cm^2], and the range of the implanted ion distribution on this plot has a maximum of $\sim 8 \times 10^4$ atoms/cm^3/atoms cm^2. Multiplying this value by the dose of 10^{15} Al$^+$/cm^2 gives $\sim 8 \times 10^{19}$ Al/cm^3 which is close to the analytical solution.

Chapter Review
The chapter began with a description of neutron–nuclear collisions, utilizing the absence of charge on the neutron to describe the interaction using a hard sphere approximation. Expressions for the energy transfer in elastic and inelastic scattering collisions were developed, and (n, 2n) and (n, γ) reactions were analyzed as well to determine the energy transferred. Table 1.2 summarizes the energy transfer and energy transfer cross sections for these types of reactions. The description of projectile–target interaction was broadened to include ion–atom and atom–atom collisions which are relevant for two important cases: ion irradiation or implantation and the interaction between atoms in a lattice after the initial collision with a neutron in reactor materials. Interatomic potentials form the basis for describing the

interaction between atoms and also for determining the energy transfer cross section. Table 1.3 summarizes the important potentials used to describe these interactions.

Collision kinematics was then used to develop a description of the orbit of colliding atoms and hence the transferred energy and the energy transfer cross section. Because there is not one single interatomic potential that describes the interaction over the entire distance (energy) range, the energy transfer and energy transfer cross sections are analyzed in various energy ranges and for various classes of interactions. Rutherford scattering is used to describe light energetic ions, and slow heavy ions, energetic heavy ions, and relativistic electrons are all treated separately. Table 1.5 summarizes the energy transfer and energy transfer cross section for various atom–atom collisions.

Energy loss theory is developed in order to determine the energy loss of energetic atoms/ions to the solid by elastic/nuclear collisions and by collisions with the electrons of the target. Collisions are analyzed in terms of their energy range for both nuclear stopping and electronic stopping. Table 1.7 summarizes the stopping powers for various types of interactions. Finally, the stopping powers are used to develop expressions for the range and projected range of ions in solids so that their penetration depth and concentration distribution can be determined.

Nomenclature

a	Screening radius
a_0	Bohr radius of the hydrogen atom
a_U	Universal screening length
A	Atomic mass, or Pre-exponential constant in Born–Mayer relation, Eq. (1.47)
b	Impact parameter
B	Constant in exponent in Born–Mayer relation, Eq. (1.47)
C	Constant in screened Coulomb potential, Eq. (1.49) = 0.8853
c	Speed of light
D	Nearest neighbor spacing between atoms
E_a	Value of E_i that yields $\rho_0 = a$
E_b	Value of E_i that gives $T \geq E_\mathrm{d}$ at $b = a$
E_d	Displacement energy
E_D	Maxwellian nuclear temperature = kT
E_f	Final energy
E_γ	Gamma ray energy
E_i	Incoming particle energy
$E^f_{\mathrm{v,i}}$	Vacancy and interstitial formation energy
$E^m_{\mathrm{v,i}}$	Vacancy and interstitial migration energy
E'_m	Kinetic energy of incoming particle in CM system
E''_m	Energy of neutron after (n, 2n) reaction
E'_M	Kinetic energy of target particle in CM system
E''_M	Energy of CM after (n, 2n) reaction

E_{R}	Rydberg energy
E_{T}	Total energy
$\bar{I}$	Excitation–ionization level
k_e	Coulomb constant
m	Mass of incoming particle
M	Mass of target
N	Atom number density
N_{p}	Peak implanted ion concentration
N_{s}	Implanted ion density in ions/unit area
p_{e}	Momentum of electron
Q	Excitation energy of nucleus
r_{e}	Nearest neighbor spacing between atoms
$\dot{r}$	Radial velocity in polar coordinates
R	Range of ion
R_{eff}	Recombination radius
R_{p}	Projected range
ΔR_{p}	Standard deviation of projected range
s	Power law exponent
S_{e}	Electronic stopping power
S_{n}	Nuclear stopping power
t	Time, or Dimensionless collision parameter, Eq. (1.142)
T	Energy transferred in collision
$\check{T}$	Minimum energy transferred
$\hat{T}$	Maximum energy transferred
$\overline{T}$	Average energy transferred
T_ℓ	Energy transferred to target atom after (n, 2n) reaction
$V(r)$	Potential energy
υ_{c}	Velocity of incoming particle in CM system
V_{c}	Velocity of target particle in CM system
υ'_{c}	Velocity of incoming particle in CM system after collision
V'_{c}	Velocity of target atom in CM system after collision
υ''_{c}	Velocity of neutron in CM system after (n, 2n) reaction
V''_{c}	Velocity of target atom in CM system after (n, 2n) reaction
V_{CM}	Velocity of CM in laboratory system
υ_ℓ	Velocity of incoming particle in laboratory system
υ'_ℓ	Velocity of incoming particle in laboratory system after collision
V'_ℓ	Velocity of target atom in laboratory system after collision
V''_ℓ	Velocity of target atom in laboratory system after (n, 2n) reaction
Z	Atomic number
β	υ/c
$\chi(r)$	Screening function
χ_U	Universal screening function
ε	Unit electronic charge
ε_0	Electric constant

$\in$	Dimensionless, reduced energy parameter, Eq. (1.139)
ϕ	Asymptotic scattering angle at infinity separation
ϕ	Scattering angle in CM system
$\dot{\psi}$	Angular velocity in polar coordinates
ψ	Scattering angle of struck atom in laboratory system
λ	Mean free path between collisions
λ_m	see Eq. (1.144)
λ'	1.309, Eq. (1.143)
μ	Reduced mass, Eq. (1.63)
$\nu(T)$	Displacement function
θ	Scattering angle in laboratory system
ρ	Distance between atom centers in a collision
ρ_e	Electron cloud density
ρ_0	Distance of closest approach, value of r when $\psi = \pi/2$
ρ_r	Dimensionless, reduced distance parameter, Eq. (1.140)
$\sigma\ (E_i)$	Total atomic collision cross section
$\sigma\ (E_i, T)$	Differential energy transfer cross section
$\sigma\ (E_i, \phi)$	Differential angular collision cross section
$\sigma\ (E_i, E_\phi, \Omega)$	Double differential collision cross section
$\sigma\ (E_i, Q_j, \phi)$	Differential angular cross section for inelastic collisions
$\sigma\ (E_i, Q_j, T)$	Differential energy transfer cross section for inelastic collisions
Ω	Solid angle into which incoming particle is scattered
$d\Omega$	Differential solid angular element
ξ_e	$Z_1^{1/6}$

Problems

1.1 A 0.5 MeV neutron strikes a target atom with mass A, which is initially at rest. Calculate the velocity and energy of both particles in the laboratory reference frame after a head-on collision for $A = 27$ (Al) and $A = 207.2$ (Pb).

1.2 A detector of 100 % efficiency (i.e., every particle entering the detector is registered) and area of 1 cm^2 is placed at a distance r from a target (taken to be of zero dimension, i.e., a point). The target is bombarded with neutrons. Assuming that only elastic scattering occurs, scattering is azimuthally symmetric, and the scattering cross section is isotropic:

(a) What is the ratio of the number of particles detected by the detector at positions 1 and 2 shown in the figure?

(b) What is the ratio of the number of particles scattered through an angular increment of 10° about $\theta_1 = 5°$ and $\theta_2 = 85°$?

(c) Repeat parts (a) and (b) assuming that instead of being isotropic, the differential scattering cross section varies as $\sigma_s(E_i, \theta) = \cos\theta$.

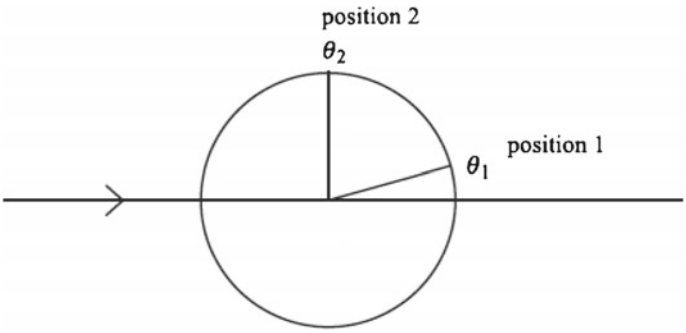

$d\theta$ = Increment of scattering angle
$d\Omega$ = Increment of solid angle about θ
θ = Scattering angle in the lab system

1.3 A Ti plate is bombarded with 10^{14} neutrons per cm^2 per second at perpendicular incidence. The entire plate is hit by the beam.

(a) Calculate the number of particles scattered per second at

(i) $85° \leq \theta = 86°$ and
(ii) $5° \leq \theta = 6°$.

The plate size is 1 cm^2 by 0.6 mm thick. Scattering is isotropic with a total scattering cross section of 2.87 barns (1 barn = 10^{-24} cm^2).

(b) The same target is bombarded with particles such that the differential angular scattering cross section is proportional to θ^2. Calculate the ratio of the atomic flux in interval (i) above to that in interval (ii). In both cases, perform full integration of the differential cross section.

(c) Approximate the integrals in (b) by assuming the differential angular scattering cross section to be constant in each integration interval and equal to the value at the interval's center.

1.4 Derive the kinematic factor K, defined as $K = E_f/E_i$, where E_i is the projectile energy before the collision and E_f is the projectile energy after the collision.

1.5 The following formula relates the scattering angles θ and ϕ in the laboratory and center-of-mass frames, respectively:

$$\tan\theta = (M/m)\sin\phi/[1 + (M/m)\cos\phi]$$

where m and M are the masses of the projectile and target, respectively. Discuss this expression for the following three cases: $m = M$, $m \gg M$, and $m \ll M$.

1.6 Derive Eq. (1.24) in the text.

1.7 Derive Eq. (1.39) in the text.

1.8 For two colliding particles write expressions for:

(a) E_T, the total energy of a system of n particles;
(b) E_{CM}, the energy of the center of mass (determined by V_{CM} and the total mass of the system); and
(c) E, the total energy in the CM system.
Show that $E = E_T - E_{CM}$ [Eq. (1.61)]

1.9 Derive a relation between b and ϕ from Eq. (1.76) for the hard sphere potential:

$$V_{HS}(r) = 0 \quad r > r_0$$
$$= \infty \quad r \leq r_0$$

Make sure your answer is correct for $b > r_0$.

1.10 As a means of describing atom–atom interaction at intermediate separation, i.e., between Coulombic repulsion and closed shell repulsion, an inverse power potential is often employed of the form

$$V(r) = \text{constant}/r^n.$$

For example, one can fit an inverse square ($n = 2$) function to the screened Coulomb potential at $r = a$ obtaining the same slope, ordinate, and curvature. This function is as follows:

$$V(r) = z_1 z_2 \varepsilon^2 a/(r^2 \exp[1]).$$

Formulate the cross sections $\sigma_s(E_i, T)$ and $\sigma_s(E_i, \phi)$ for atom–atom interactions obeying the inverse square potential function.

1.11 Compare your result in Problem 1.10 to that obtained using a Born–Mayer potential and a simple Coulomb potential. Comment on the similarities and differences.

1.12 Calculate the average energy transfer from a 100 keV Ni atom colliding with another Ni atom, using:

(a) The hard sphere potential and
(b) The inverse square potential.

1.13 Explain, in physical terms, why the scattering cross section resulting from Coulombic repulsion depends on the transferred energy, T, while that for neutron–nuclear interaction does not.

1.14 Assuming a pure Coulomb potential, determine the distance of closest approach for a 100 keV boron atom on silicon for an impact parameter, $b = 1$ nm. What is the significance of your answer?

1.15 1 MeV Al^+ ions are accelerated toward a pure Ni target. The ions are directed normal to the sample surface.

(a) Calculate the total path length and provide an estimate for the mean projected range of the ions.
(b) For a dose of 10^{16} ions/cm^2, estimate the maximum Al concentration and the FWHM of the Al distribution. Use $S_e(E) = k'E^{1/2}$, where $k' = 2 \times 10^{-16}$ eV$^{1/2}$ cm^2.

1.16 A 10 MeV Si ion penetrates a Si crystal.

(a) Calculate its energy as a function of distance traveled and its penetration depth. Assume that electronic stopping dominates.
(b) Write an expression for the depth distribution of implanted Si ions and give the straggling.

1.17 Calculate the energy threshold above which the Rutherford scattering cross section can be used for: (i) near head-on collisions and (ii) all collisions of He^{++} and H^+ in Si and Pd.

1.18 2 MeV He^{++} ions are backscattered ($\theta = 180°$) off of a 25-nm-thick gold foil. Determine the highest and lowest energy values of the backscattered ions as measured in a detector placed at 180° with respect to the incoming beam. Use $k = 0.14 \times 10^{-15}$ eV$^{1/2}$ cm^2.
Determine the stopping power by interpolation or extrapolation based on the following values of $1/N(dE/dx)$ (in eV/(10^{15} atoms/cm^2)):

Energy (MeV):	1.6	2.0
Au	122.3	115.5
Al	47.5	44.25

1.19 Assume the stopping power can be described by the following function:

$$S = C + KE^{1/2} \text{ where } C \text{ and } K \text{ are constants.}$$

(a) Derive an equation for the particle range as a function of energy.
(b) Does the range increase or decrease as:

(i) Energy increases;
(ii) K increases; and
(iii) C increases.

1.20 Which increases the high-energy electronic stopping power the most, increased charge, energy, or mass of the projectile ion?

1.21 A 2 MeV proton travels through lead.

(a) Assuming elastic collisions, calculate the maximum energy that can be transferred from the proton to the lead.

(b) What energy would a Pb ion need to have the same maximum energy transfer in a Pb–Pb collision as the proton–Pb collision in part (a)?

1.22 An Fe particle is fired at a block of natural uranium. To get the Fe as close to the uranium particle as possible, would you be better off using a higher charge state of Fe or a lighter isotope? Assume Coulomb potentials can be used.

1.23 A thin film containing F^{19} is bombarded with 1.85 MeV protons. The following reaction takes place:

$$F^{19} + p \rightarrow O^{16} + \alpha.$$

The reaction has a Q value of 8.13 MeV. After interaction, an alpha particle is seen to emerge at a right angle to the incident proton beam. What are the energies of the alpha particle and the oxygen atom? What is the maximum energy each of these particles could transfer to a stationary Fe atom?

1.24 A helium atom at 1 MeV is sent into iron. Assuming the electronic stopping cross section is a constant (88×10^{-5} eV cm^2), what is the energy of the helium atom after it travels 500 nm? If the He atom collides with an Fe atom after traveling 500 nm, what is the maximum energy transferred? Assume an atomic density of 8.5×10^{22} atoms/cm^3 for Fe. Was an assumption of constant stopping power valid?

References

1. Ullmaier H, Schilling W (1980) Radiation damage in metallic reactor materials. In: Physics of modern materials, vol I. IAEA, Vienna
2. Lamarsh JR (1971) Introduction to nuclear reactor theory. Addison-Wesley, Reading, MA
3. Doran DG (1972) Neutron Dispalcement Cross Sections for Stainless Steel and tantalum based on a Lindhard model. Nucl Sci Eng 49:130
4. Odette GR (1972) Energy Distribution of neutrons from (n,2n) reactions. Trans Am Nucl Soc 15:464
5. Segev M (1971) Inelastic matrices in multigroup calculation, ANL-7710. Argonne National Lab, Argonne, IL, p 374
6. Evans RD (1955) The atomic nucleus. McGraw-Hill, New York
7. Chadderton LT (1965) Radiation damage in crystals. Methuen, London
8. Born M, Mayer JE (1932) Zur gittertheorie der ionenkristalle. Z Physik 75:1
9. Firsov OB (1957) Calculation of the interaction potential of atoms for small nuclear separations. Zh Eksper Teor Fiz 32:1464
10. Firsov OB (1957) Calculation of atomic interaction potentials. Zh Eksper Teor Fiz 33:696
11. Brinkman JA (ed) (1962) Radiation damage in solids. Academic, New York
12. Abrahamson AA (1963) Repulsive interaction potentials between rare-gas atoms. Homonuclear two-center systems. Phys Rev 130:693
13. Thompson MW (1969) Defects and radiation damage in metals. Cambridge University Press, Cambridge

14. Lindhard J, Nielsen V, Scharff M (1968) Approximation method in classical scattering by screened Coulomb fields. Mat Fys Medd Dan Vid Selsk 36(10):1–32
15. Winterbon KB, Sigmund P, Sanders JB (1970) Spatial distribution of energy deposited by atomic particles in elastic collisions. Mat Fys Medd Dan Vid Selsk 37(14):1–73
16. Lindhard J, Scharff M, Schiott HE (1963) Range concepts and heavy ion ranges. Mat Fys Medd Dan Vid Selsk 33(14):3
17. Lindhard J, Winther A (1964) Stopping power of electron gas and equipartition. Mat Fys Medd Dan Vid Selsk 34:1
18. Littmark U, Ziegler JF (1980) Handbook of range distributions of energetic ions in all elements. Pergamon, New York
19. Nastasi M, Mayer JW, Hirvonen JK (1996) Ion-Solid Interactions: fundamentals and applications. Cambridge University Press, Cambridge
20. Ziegler JF (2015) SRIM The stopping and range of ions in solids. IIT Co. (www.srim.org)